OPEN ACCESS
Journal of Innovative Optical Health Sciences
Vol. 14, No. 4 (2021) 2130003 (28 pages)

DOI: 10.1142/S1793545821300032

World Scientific
www.worldscientific.com

Plasmonic nanoparticles and nucleic acids hybrids for targeted gene delivery, bioimaging, and molecular recognition

Timofey Pylaev[*,†,‡,¶], Elena Avdeeva[*] and Nikolai Khlebtsov[*,§]
[*]*Institute of Biochemistry and Physiology of Plants and Microorganisms Russian Academy of Sciences, Saratov 410049, Russia*
[†]*Razumovsky Saratov State Medical University, Saratov 410012, Russia*
[‡]*Federal Center of Agriculture Research of the South-East Region, Saratov 410010, Russia*
[§]*Saratov National Research State University Saratov 410012, Russia*
[¶]*pylaev_t@ibppm.ru*

Received 19 May 2021
Accepted 22 May 2021
Published 23 June 2021

Promising biomedical applications of hybrid materials composed of gold nanoparticles and nucleic acids have attracted strong interest from the nanobiotechnological community. The particular interest is owing to the robust and easy-to-make synthetic approaches, to the versatile optical and catalytic properties of gold nanoparticles combined with the molecular recognition and programmable properties of nucleic acids. The significant progress is made in the development of DNA–gold nanostructures and their applications, such as molecular recognition, cell and tissue bioimaging, targeted delivery of therapeutic agents, etc. This review is focused on the critical discussion of the recent applications of the gold nanoparticles–nucleic acids hybrids. The effect of particle size, surface, charge and thermal properties on the interactions with functional nucleic acids is discussed. For each of the above topics, the basic principles, recent advances, and current challenges are discussed. Emphasis is placed on the systematization of data over the theranostic systems on the basis of the gold nanoparticles–nucleic acids hybrids. Specifically, we start our discussion with observation of the recent data on interaction of various gold nanoparticles with nucleic acids. Further we describe existing gene delivery systems, nucleic acids detection, and bioimaging technologies. Finally, we describe the phenomenon of the polymerase chain reaction improvement by gold nanoparticle additives and its potential underlying

[¶]Corresponding author.

mechanisms. Lastly, we provide a short summary of reported data and outline the challenges and perspectives.

Keywords: Gold nanoparticles; delivery; DNA detection; bioimaging.

1. Introduction

The use of nanoparticles, especially gold nanoparticles (AuNPs) in various biomedical fields[1] including targeted delivery,[2–4] vaccine development,[5] and biosensorics,[6] was greatly expanded during the last two decades. Since then several reliable methods for high-yielding, reproducible, and controllable synthesis of AuNPs with desired properties have been developed.[7–9] Chemically fabricated AuNPs offer several interesting physical and chemical attributes: (a) variety of sizes, tunable surface charges and shapes[10]; (b) chemical and thermal stability[11]; (c) high surface-to-volume ratio; (d) unique optical and electronic features due to the strong localized surface plasmon resonance (LSPR) absorption and scattering cross sections; (e) high biocompatibility and low immunogenicity.[12] These properties determine the use of AuNPs as promising building blocks for further functionalization with biomolecules of interest. During the past decades, a broad list of functional hybrids based on the conjugated AuNP with antibodies,[13,14] enzymes,[15,16] peptides,[17] and nucleic acids (NA)[18–21] have been developed for various uses. Specifically, the AuNP–NA hybrids are one of the most promising, and present the current interest in this review. Indeed, more than 1000 experimental and review studies with AuNP–NA hybrids are published annually since 1996, when Mirkin and co-workers introduced the concept of the cross-linking biospecific aggregation of the AuNPs functionalized with oligoDNA.[22] Following this concept, similar approaches were developed and applied in nano-assembly,[23–25] environmental monitoring,[26,27] disease diagnosis,[28–30] cell imaging,[31–33] and drug delivery[34,35] due to their unique distance-dependent optical properties, effective programmable binding, rapid cell uptake, and low innate immune responses.[36–38]

Nevertheless, many tasks concerning the topic remain unclear. Specifically, there is no universal approach for programmable functionalization of different AuNPs with NA with desired parameters. The current mechanisms for cellular uptake, the pathways, and intracellular behavior of AuNP–NA hybrids are still unclear. The problems of analytical range, the specificity, sensitivity, and selectivity in aggregation-based sensors with AuNP–NA hybrids are worth further investigations before being transferred to clinical usage. Thus, we hope that the present review, being aimed at systematic and critical observation of the recent studies, will be helpful in the context of the mentioned challenges. This mini-review is divided into several sections, starting with brief outline of the major features of the AuNPs and NA which are important to their rational assembly into functional nanohybrids. The following sections are devoted to the applications of AuNP–NA hybrids in biosensing, bioimaging, intracellular delivery, and polymerase chain reaction (PCR) improvement. For each of the above topics, the basic principles, recent advances, and current challenges are discussed.

2. The Building Blocks of NA-Plasmonic Nanohybrid-Based Technologies

2.1. *Functional NA*

Chemically, DNA and RNA are heteropolymers, consisted of repeating units, called nucleotides. All nucleotides in turn include a pentose sugar, a phosphate group, and a nitrogenous base. DNA differs from RNA. The structural "backbone" sugar is deoxyribose for DNA and ribose for RNA.[39] The thymine base is substituted in RNA with the corresponding base uracil. Finally, DNA has double-stranded (ds) helix-shaped second structure, like a flexible ladder twisted in opposite directions at both ends, while RNA has single-stranded (ss) helix structure. While DNA is concerned only with information storage, different types of RNA, namely messenger RNA (mRNA), transfer RNA (tRNA), ribosomal RNA (rRNA), and small interference RNA (siRNA) assume different functions in the living cells.[40] Thanks to the next-generation sequencing (NGS) technologies[41] associated with improvements in bioinformatics techniques and

software which allow to obtain, analyze, and manipulate NA sequences in different ways. DNA reading by NGS when combined with DNA synthesis technologies[42] forms the basis for the development of modern NA-based engineered systems,[43] such as the AuNP-based detection[44] and delivery[45] systems (Figs. 1(h)–1(m)). The key component of such strategies is the ability of NA to be incorporated or attached to the AuNP surface simultaneously with vast number of different functional groups like organic molecules (e.g., fluorescent dyes), polymers, proteins, and other NPs. Typical building blocks[46] used in the AuNP-based strategies are bare synthetic mono- and oligonucleotides,[47] aptamers,[48,49] DNAzymes,[50] or modified with peptides (PNA),[51] sugars,[52] and lipids.[53] As molecular cargoes, several types of functional NA, such as cytosine-phosphate-guanine (CpG) sequences, antisense sequences,[54,55] siRNA, miRNA, etc., have been engineered to the DNA nanoarchitectures.[56] DNA molecules possess well flexibility and programmability eager to be used as alternative templates for NP assembly. The configurations of DNA-based plasmonic heterostructures can be controlled by adjusting the structural parameters related to DNA molecules, involving dimers, trimers, pyramids, chains, and core-satellites.[46] A prerequisite for building plasmonic metal NP heterostructures is the stable modification of DNA on NPs for DNA hybridization. Various functional groups, such as sulfhydryl, amino, carboxyl, and hydroxyl (Fig. 1(c)), can be attached to the ends of DNA sequences.[42]

2.2. *Plasmonic nanoparticles: Tunable parameters towards multifunctional modalities*

The intense electromagnetic enhancement gives rise to intense optical responses, which is dependent on sizes, shapes, and even the orientation of constituent NPs.[57] Plasmonic metallic NPs, especially AuNPs and AgNPs, possess tunable LSPR over a broad spectral range from the visible to the NIR regions and display better plasmonic activities than copper and aluminum NPs. Wet chemistry-based bottom-up approaches allow to synthesize plasmonic NPs with desired geometry (Fig. 1(a)) such as nanospheres, nanorods (NRs), nanostars, nanocubes, nanoflowers, nanobipyramids, core–shell NPs, and nanodumbbells.[58] The sizes, aspect ratios,

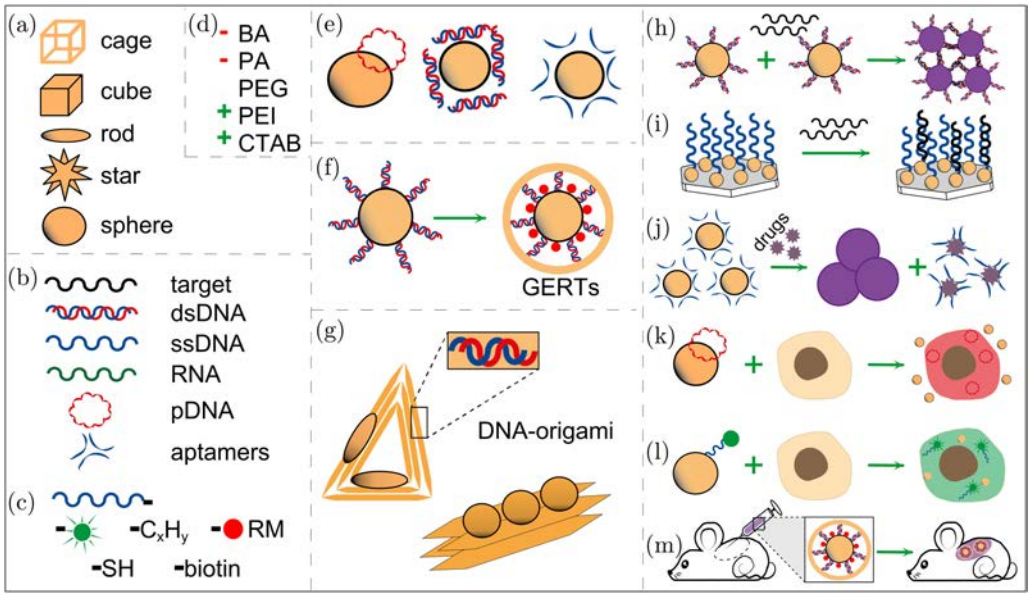

Fig. 1. Schematic overview of theranostic systems based on the AuNPs complexed with physically adsorbed NA (e) or AuNPs with covalently bonded NA (f), (g), with varying parameters: core shapes (a), surface capping ligands (d), functional NA probes (b), Raman or fluorescent reporters (c). Samples of *in vitro* and *in vivo* applications for biomolecular sensing (h)–(j), targeted delivery and bioimaging (k)–(m). Reproduced from Refs. 59 and 60; Repreduced with permissions from Refs. 61 and 62. The used abbreviations are BA: bromosalicylic acid, PA: polyacrylic acid, PEG: polyethyleneglycol, PEI: polyethylenimine, CTAB: cetyltrimethylammonium bromide, dsDNA: double stranded DNA, ssDNA: single-stranded DNA, RM: Raman molecule and GERT: gap-enhanced Raman tag.

and surface roughness can be well controlled by adjusting the growth parameters (pH, ionic strength, reaction times, ligands, etc.).

The modified AuNPs with NA molecules should possess stability[63] for long-term storage and unchanged properties in complex environment conditions.[64] Particularly, the subjection to the influence of external environment changes, such as complex biofluids, high ion strength solution, and freeze-drying processes[65] should retain the initial properties. To improve the stability of DNA–AuNPs conjugates, several strategies were proposed[66–71] that utilize different modifications of the AuNP surface, oligoDNA chains or by varying the reagents and conditions of the conjugation procedure. The commonly used thiolated molecules for AuNP surface modification, including a nonionic thiolated PEG, mercaptopropionic acid, glutathione, dihydrolipoic acid, cysteine, and cysteamine, exhibited very little tolerance to pH or ionic strength with the exception of the thiolated PEG.[72] Further investigations by Hinman *et al.*[67] showed that the colloidal stability of DNA–AuNPs conjugates can be remarkably improved by utilizing the oligonucleotides with end linkers of poly-thymine bases. Specifically, the AuNPs modified with T_{20}-oligs demonstrated high salt tolerance up to 6 M NaCl, with maintained stability during freeze-thawing and lyophilization cycles. The oligoDNA modified by alkanethiols of varying chains are also considered as effective end linkers that improve loading capacity[73] by reduced stiffness of bonded oligoDNA. Another strategy is based on capping the AuNP surface with surfactants[74] (Fig. 1(d)) prior to attaching the thiolated DNA. Such approach can be helpful, for example, for modifying the AuNRs which are capped by CTAB bilayer in as-prepared colloids. It was reported that the replacement of undesirable CTAB molecules by bromosalicylic acid[75] sufficiently improved the subsequent attachment of thiolated DNA. The other reported studies for AuNRs conjugation with thiolated DNA are based on round-trip phase transfer,[76] vinyl carboxylate-modified cationic surfactant in combination with amino-modified DNA molecules,[77] direct DNA functionalizing via salt aging,[78] low pH[79] or low temperature,[80] and ligand-exchange approach using poly-(vinylpyrrolidone) as intermediate.[81] Liu and co-workers[74] developed a bioconjugate strategy based on the combination of polydopamine (PDA) shell and DNA linker. The obtained DNA linked DNA–Au@PDA NPs showed the colloidal stability in high ionic strength solution and complex systems (such as human serum and cell culture supernatant). Moreover, the nanoparticles still maintained good dispersion after multiple freeze-thaw cycles. Through investigating the effect of different modification assay based on various polymers and DNA linker (T_{20}, C_{20}, and A_{20}) on the stability of DNA functionalized Au@PDA NPs, it was presumed that the high stability of DNA–Au@PDA NPs may be attributed to increasing the electrostatic and steric repulsions among nanoparticles through PDA shell and DNA linker. However, the utilization of surfactants with potential biotoxicity gain limits for further biomedical applications of DNA–AuNPs conjugates. In this regard, surfactant-free strategies can be suggested as a sophisticated alternative for obtaining stable DNA–AuNPs.[71] Small peptides can be considered as capping agents for AuNPs thus realizing in a two-step loading procedure of thiol-DNA. Specifically, Carter and LaBean[82] proposed a combined approach that utilizes a synthetic gold-binding peptide, selected from a combinatorial library, covalently bonded with oligoDNA. It allowed the self-assembling of DNA structures with defined final spatial arrangement. The peptides bonded on the AuNPs through Au–N bonds formed negative surface charge at pH 7.4, thus generating a uniformly charged layer to enhance particle stability.

Nevertheless, despite the promising results of recent studies presented above, the problem of developing a simple, inexpensive, and universal bioconjugation strategy that could improve the stability of DNA–AuNP hybrids in solutions with high ionic strength and complex systems is still open and requires further investigations for better understanding of the stated circumstances.

2.2.1. *AuNP geometry variations and the dimensional orders of DNA assemblies*

Individual DNA strands can serve as linkers to assemble AuNPs into well-defined plasmonic nanostructures based on their highly specific base-pairing ability. Early examples can date back to the year 1996, when Mirkin's[22] and Alivisatos'[83] group independently published two papers. The former synthesized two types of polyvalent DNA–AuNP conjugates that have complementary DNA sequences on the surface of AuNPs, which readily form macroscopic colloidal crystal lattices upon

hybridization in solution; the latter employed a DNA duplex to link two separate AuNPs in a predefined distance.[84] Later studies reported successful synthesis of heterodimeric and heterotrimeric AuNPs with controllable spatial arrangement.[85] To date, only few types of AuNPs with different geometries have been demonstrated to be modified with thiol DNA nanoplates,[86,87] nanocubes,[88] nanopolyhedra,[89] nanorods (AuNRs).[90–94] While a few demonstrations of DNA−AuNRs have been occasionally reported,[95] they often do not provide a general synthesis strategy for DNA conjugation and a consistent set of observation of their cooperative assembly properties.[75]

Mirkin and coworkers recently synthesized a range of Au superlattices including NRs, triangular nanoprisms, rhombic dodecahedra, and octahedral with the assistance of DNA linkers.[89] They also demonstrated that the superlattice dimensionality, crystallographic symmetry, and phase behavior of these crystalline structures, named DNA-origami (Fig. 1(g)),[97] were highly dependent on both the nanoparticles' shape and the sequence length of DNA linkers.[98] Later, Li *et al.* observed plasmonic circular dichroism (CD) responses in a DNA-linked AuNR system.[99] By tuning the thermal response of DNA linkers, they obtained the reversible plasmonic CD upon temperature-dependent assembly and disassembly of AuNRs. Using a similar strategy, they also reported a strong and reversible CD response by assembling helical DNA and Au nanobipyramids. More recently, Xu and coworkers demonstrated that AuNRs could be assembled via a PCR process to DNA-bridged chiral systems.[100]

2.2.2. *DNA–AuNP hybrids combined with fluorophores and/or Raman reporters*

The nanoprobes for surface-enhanced Raman scattering (SERS) applications that combine metallic NPs and specific Raman reporter molecules called "SERS tags"[101] offer several attractive advantages over other optical probes such as fluorescent probes. In particular, these nanoprobes are inherently suitable for multiplex analysis because of their Raman spectral bands with narrow line widths and fluorescence bands with wide line widths.[102] Nevertheless, research in developing SERS nanoprobes has fallen behind that of other nanoprobes, such as quantum dots and dye-doped nanobeads.[101] Thus far, very few SERS nanoprobes have been used for multiplex analysis of different types of bioactive molecules (Fig. 2), although there are ever-increasing demands for developing SERS nanoprobes to improve multiplex analytical performance for molecular diagnostics and bioimaging applications (Fig. 3). One important reason for this decline is that the direct synthesis of nanotags with strong and stable SERS signals remains highly challenging.[103] More recent advances have shed new light on the direct synthesis of uniform core–shell nanostructures with interior nanogaps for stable SERS enhancement, also called gap enhanced Raman tags (GERTs).[104] Once the Au cores are functionalized by RM molecules-tethered oligoDNA, thus obtained GERTs show strong and quantitative SERS signals for cell bioimaging, *in vivo* SERS-mapping of model cancer tumors, or for chemical detection purposes (Figs. 3(g)–3(j)). Lim and co-workers introduced the synthetic strategy based on the anchored DNA staples on the AuNP cores that form the interior nanogaps (Fig. 2(a)).[105] Different parameters of the synthetic procedure, such as DNA base, length, sequence, and grafting density were varied in further investigations, to reveal the effects of AuNP surface modification with thiolated DNA on the formation of the interior nanogap.[106,107] In another study Lee and coworkers proposed a method for controlled dealloying growth of bimetallic particles[110] with introduced nanogap or the so-called "nanosnowman" structures (Fig. 2(b)). In brief, the core–shell Au/Ag alloy NPs were formed by co-reduction of AuNP seeds, while the selective dealloying reaction through Fe^{3+} oxidation of Ag to Ag^{+} caused the accumulation of vacancies near the Au core surface, thus forming the interior nanogap. The measured SERS signal of various RM attached to the nanosnowman revealed about 50 times higher SERS intensity compared to that of the corresponding shell-less AuNPs or gap-less NPs. These results clarify the major role of interior nanogap in the electromagnetic field enhancement and thereby SERS intensity of Raman-active molecules. Zhang *et al.*[108] proposed a similar strategy for GERTs synthesis using the AuNR core and Ag shell formed via galvanic replacement. The tuning of gap size ranging from ~ 2.5 nm to ~ 3.3 nm was realized by adjusting the amount of added $AgNO_3$ during the shell formation. The authors demonstrated a proof-of-concept theranostic application of the GERTs doped with antitumor drug Doxorubicin and functionalized with specific recognizing aptamer: a quantitative

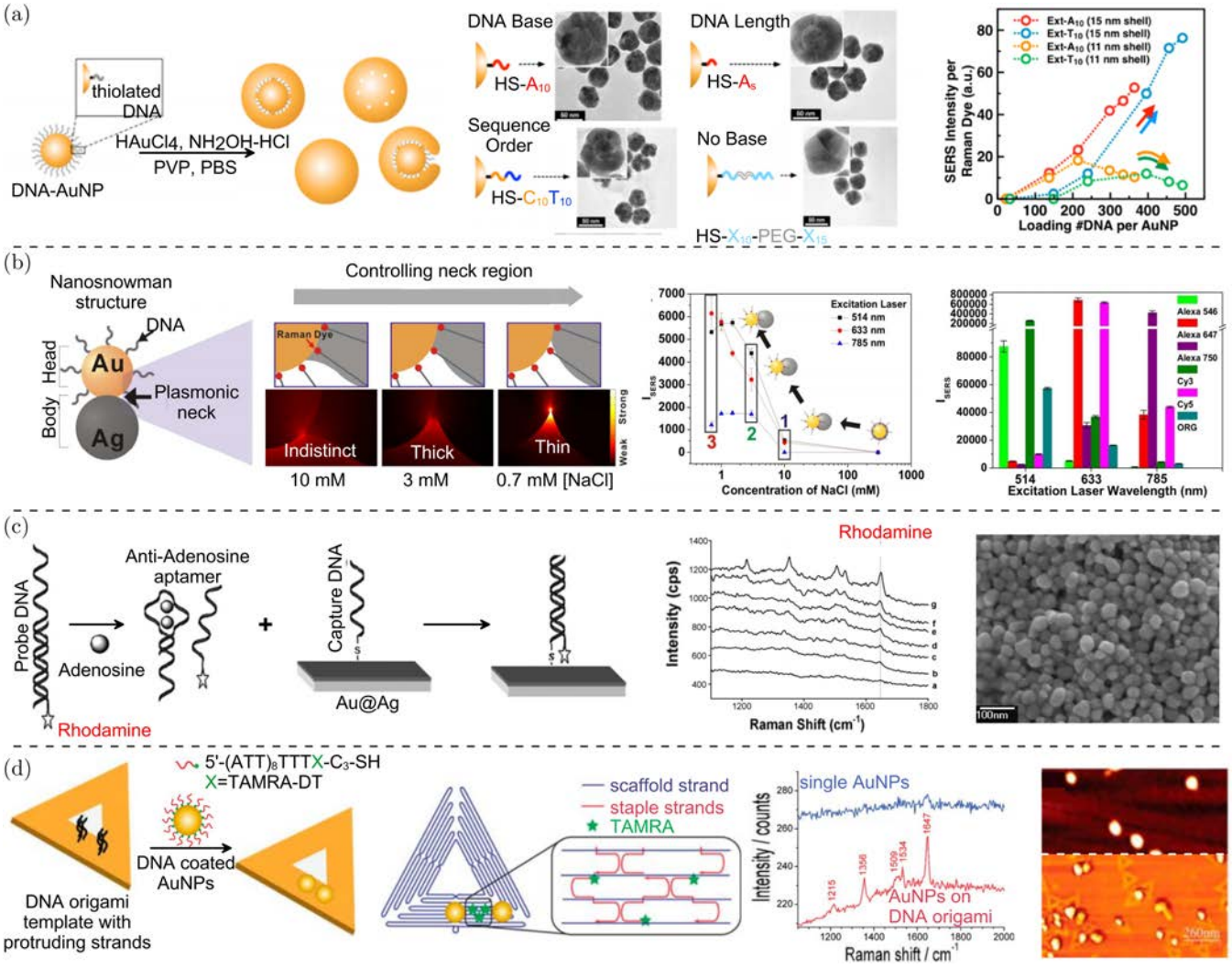

Fig. 2. SERS-sensors based on the AuNP–DNA hybrids. (a) Core–shell GERTs with interior gaps formed by oligoDNA anchors. SERS response is controlled by the nucleobase composition, length, sequence order, loading density, and Au shell thickness. Reproduced with permissions from Ref. 107. (b) Bimetallic Au–Ag "nanosnowmen" with neck regions controlled by oligoDNA spacers and NaCl concentrations. SERS response can be adjusted for different Raman dyes and excitation lasers. Reproduced with permissions from Ref. 110. (c) Au@AgNP–DNA modified films and anti-adenosine aptamers for SERS detection of adenosine with nanomolar sensitivity. Reproduced from Ref. 111. (d) SERS-active DNA origami triangles decorated with AuNPs and embedded TAMRA dye. Reproduced with permissions from Ref. 112.

SERS detection of as low as 20 MCF-7 cells in a blood mimicking fluid, and a selective cell killing via controlled heating.[108] Another strategy, introduced by Yang and co-workers,[109] was based on plasmonic Raman tags covered with three-dimensional (3D) DNA walker. These tags were used for quantitative SERS sensing of *Salmonella typhimurium* with LOD as low as 4 CFU/mL. However, the authors reported that the proposed method was limited for multiplex simultaneous detection of several bacterial species.[109]

Despite different SERS tags were recently developed and used in proof-of-concept applications, there is no universal strategy to the date for obtaining SERS-active nanostructures with desired and tunable parameters that would match all requirements. Along with the limitations of SERS tags, other complicated tasks should be addressed to the improvement of detection system, specifically, reducing the operating time, enhancing the spatial resolution, the problems with detecting large-scale and moving samples, such as living organisms. Therefore, the SERS-based techniques are still remaining challenging and need further investigations.

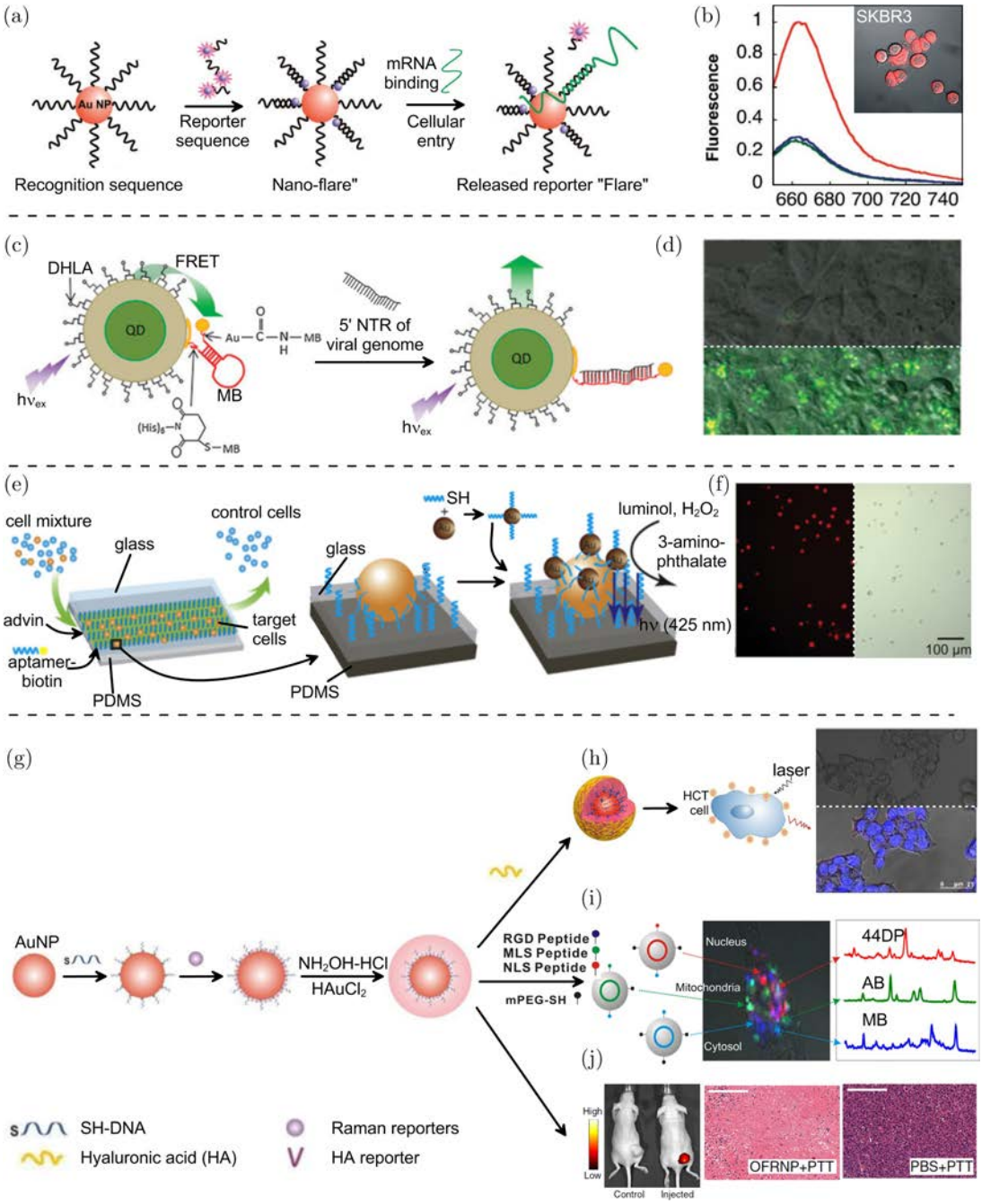

Fig. 3. DNA–AuNP hybrids for fluorescent and Raman bioimaging. (a) "Nano-flares" — AuNPs with bonded probe DNA hybridized with Cy5-labeled oligoDNA reporter, which can be displaced by the target. Fluorescence spectra of bare nano-flares (green), with added 1 nM complementary target sequences (red) and nontarget sequences (blue). The inset image shows the SKBR3 cells labeling. Reproduced with permissions from Ref. 114. "Molecular beacons" — DNA probes with QDs and AuNP quenchers (c) for *in situ* viral RNA detection in the infected cells (d). Reproduced from Ref. 116. Aptamer-based arrays (e) for selective cell capturing and chemiluminescent detection (f). Reproduced with permissions from Ref. 117. (g)–(j) Raman mapping of cancer cells using GERTs with oligoDNA spacers. (g) General scheme for GERTs synthesis. (h) Hyaluronic acid-capped GERTs with incorporated fluorophores for confocal microscopy and Raman dual imaging of HCT116 cells. Reproduced from Ref. 118. (i) GERTs with three different RM and recognizing antibodies against mitochondria, cytosol, and nucleus. Raman images overlaid with bright-field images of single HSC-3 cell. Red, green, and blue colors represent the Raman intensities from 785, 1450 and 1004 cm^{-1}, respectively. Reproduced with permissions from Ref. 119. (j) *In vivo* tumor imaging and photothermal therapy (PTT). NIR fluorescence images of ovarian cancer xenograft mouse after 48 h i.v. administration of DylightTM-780 labeled DNA (left, control), and GERTs (right). The tumor necrosis with the injected GERTs after PTT. Reproduced from Ref. 120

Apart from the development of SERS-based sensors, AuNPs and NA hybrid nanostructures can be used as fluorescent labels with high-performance parameters. Due to the special electronic properties, AuNPs can act as "superquenchers" for fluorescence via long-range resonance energy transfer.[113] The Mirkin group developed DNA–AuNP complexes termed as "nano-flares" (Fig. 3(a)) for sensitive detection of ATP and mRNA in living cells.[114] Wu and co-workers developed a DNAzyme–AuNP probe-based assay to detect uranyl ion in living cells.[115] The fluorescence is recovered by addition of UO_2^{2+} that causes the cleavage of fluorophore-labeled substrate strands by DNAzyme, releasing the shorter strand from AuNPs. Moreover, it was demonstrated that this approach can be potentially used *in vivo* as a metal ion sensor.

3. AuNP-Based Gene Delivery Systems

3.1. *Gene therapy: General remarks, challenges, and future perspectives*

The influence of cell barriers on the free administration of NA imposes serious restrictions to the developing gene delivery systems and their transfer from model issues to the real clinical practice. In addition to the extracellular barriers, mainly apart from the specific macrophage immune reactions and digestive enzyme systems, the known intracellular barriers such as the cell membrane, the systems of lysosomal degradation, and endosomal escape, sufficiently hinder the expression of the internalized genes. The penetration of large molecules in the living eukaryotic cells is realized by endocytosis, subdivided into phago- and pinocytosis. The ability to phagocytose has several types of cells, such as macrophages, neutrophils, and dendritic cells.[121] On the contrary, the pinocytosis pathway is presented in almost all animal cells, subdivided into clathrin- and caveolin-mediated or non-clathrin endocytosis,[122,123] macro- and micropinocytosis.[124]

Despite the vast list of research studies on the gene delivery was carried out, the exact mechanisms and key factors involved in the administration of extracellular NA, as well as characteristic responses from the cell, have not yet been determined.[125–127] In this regard, it makes sense to further investigate NA delivery methods, their underlying mechanisms, advantages, challenges, and future perspectives. Figure 4 shows schematically the most well-known delivery systems and their principles of operation; a more detailed description is presented in the following subsections.

3.2. *AuNP-based nanocarriers*

The gene carriers based on the metallic NPs mainly AuNPs[130] are considered to be one of the most promising due to the unique properties of AuNP, such as simplicity and scalability of the synthesis, tunable plasmonic properties, low immunogenicity, bioinertness,[131] and the ability to effectively complexing the cargo NA molecules. Due to these promising features, a broad number of AuNP-based nanocarriers was developed for efficient *in vitro* and also *in vivo* gene delivery.[132] In the recent reviews, the summarized data on the AuNP-based delivery techniques is given along with the designation of the challenges and perspectives.[49,127,133,134] The discussed issues are the rational design of AuNPs with encapsulated or adsorbed cargo molecules, the effects of size, charge, and surface ligands to better undergo the cell barriers. Among all known to the date strategies, the major interest is concerned to the delivery of the clustered system of regularly interspaced short palindromic repeats (CRISPR)-CRISPR-associated nuclease 9 (CRISPR-Cas9),[135] obtained from the acquired immune system in bacteria and archaea.[136] This system provided a new tool for the precise manipulation with genome with regard to the therapeutic outcome. The advantage of CRISPR, which has made it an easy and flexible tool for various genome editing purposes (Fig. 5), is that it is a single protein complex (Cas9) with two short RNA sequences functions as a site-specific endonuclease.[137] The CRISPR-Cas9 system demonstrates a new era in gene defect correction for the treatment of numerous human diseases with gene therapy,[138] but a number of technical problems related to the accuracy and efficiency still need to be solved, along with various Cas9-mediated off-target events (uncontrolled repair and reorganization or genome modeling),[139,140] with the development of the methods for cell cycle synchronization, ways to control the bypassing time of Cas9 protein complexes and targeting a nontarget DNA strand.[141,142] In the short list given in Table 1, we refer to a few recent studies on the AuNP-based nanocarriers, that considered to be the most promising with regard to further clinical implementation.

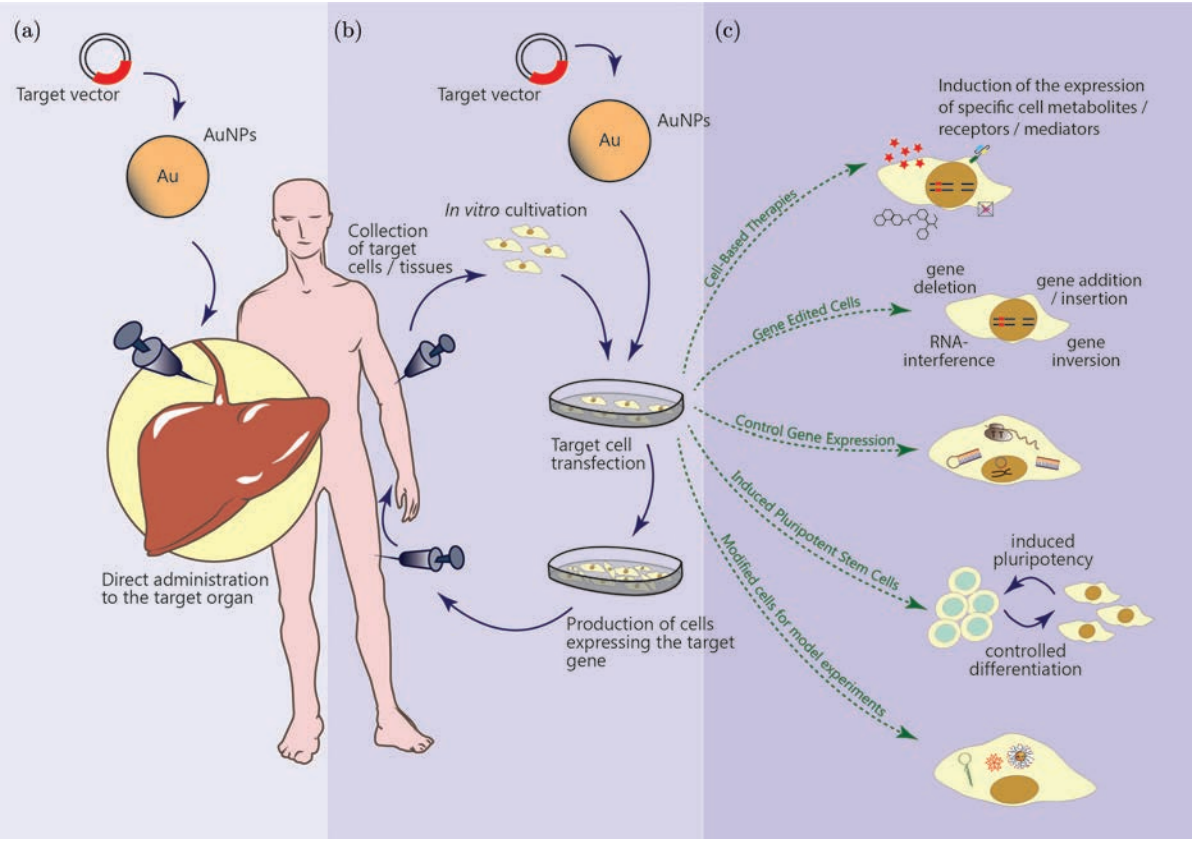

Fig. 4. Schematic overview of the AuNP-based carriers for gene therapy. Basic concepts for direct *in vivo* implementation (a), or indirect, with additional *in vitro* modification of target cells (b). The samples of therapeutic applications with reprogrammable gene-edited cells (c). Reproduced with permissions from Refs. 128 and 129.

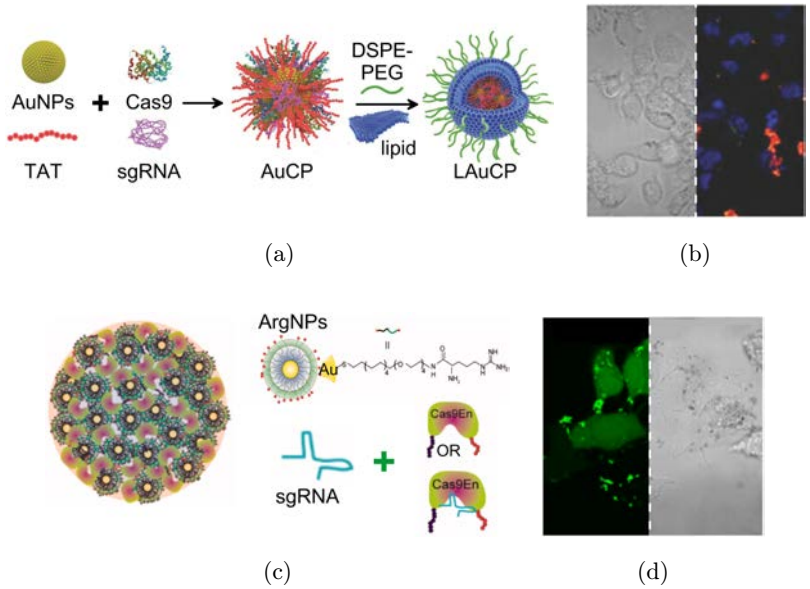

Fig. 5. AuNP-based nanocomposites for CRISPR-Cas9 delivery. (a) Scheme for the assembling of the AuNP-lipid@Cas9-Tat-peptide-plasmid composites (LAuCP). (b) Confocal images of the internalization the Cas9 protein/sgPlk1 plasmid formulations by A375 cells. Blue: nucleus, Green: FITC-Cas9 protein, Red: Cy3-sgPlk1 plasmid. Reproduced from Ref. 143. (c) Arginine@AuNP assembled polycomposites for Cas9En delivery via membrane fusion. (d). Cholesterol-dependent membrane fusion-like delivery of Cas9En-ribonucleoproteins. Reproduced with permissions from Ref. 144.

Table 1. Intracellular gene delivery systems based on AuNP nanocarriers.

Shape	Size (nm)	Capping ligand	Cargo	*In vitro* Cell line	*In vivo* model	[a]Efficacy	[b]Viability	Year, Ref.
Sphere	10	PEI	pDNA	B16F10, HeLa, CHO	BALB/C nude mice	14	n.d.	2016, 145
Star	80	lauryl sulfo-betaine or TritonX-100	siRNA	MCF-7	—	50	80	2017, 146
Sphere	20	n.d.	pDNA	MTH53A	—	50	35	2011, 147
Sphere	12	Folic acid	pDNA	MCF-7, A549	nude mice	85	n.d.	2017, 148
Composite	218	BSA	IR780 dye	MGC-803,	nude mice	80	96	2019, 149
Sphere	15	oligoDNA	Cas9 pDNA	HEK293, Human embryonic stem cells,	C57BL mice	n.d.	83	2017, 150
Composite	475	Arginine	Cas9, labeled dextrane	HeLa	—	90	n.d.	2017, 144
Cluster	2.3	PAMAM, mPEG-COOH	CpG	BMDC	C57/BL6 mice	75	75	2020, 151
Sphere	40	Chitosan	siRNA	H1299-eGFP	—	34	80	2021, 152

[a]The data is given in the percent of transfected cells counted by fluorescent images processing or by flow cytometry.
[b]The data is given in the percent and represents the results of live-dead staining and fluorescent bioimaging or cell respiratory assays.

3.3. *Plasmonic assisted laser transfection (optoporation) systems*

The delivery of external cargoes due to the increased permeability of the cell membrane induced by the light exposure is called optoporation, optoinjection, or laser infection. There are three main types of optical delivery systems. The first of them, direct photoporation,[153] is performed by narrowly focused laser irradiation. The second type is optoporation mediated by photosensitizing NPs,[154] which efficiently absorb the energy of laser radiation and cause local damage to the lipid bilayer due to photothermal effects. The third approach is based on the photothermal effects of photosensitive substrates[155,156] for the cultivation of cells that are activated by laser irradiation.

3.3.1. *AuNP suspensions as local laser-induced heat transducers for increased cell membrane permeability*

It should be noted that fast and ultrashort lasers are very expensive and require careful optical alignment. In this regard, the further development of optoporation methods is associated with the use of sensitizing NPs or micro- and nanostructured substrates.[157] In general, the procedure is as follows: cells are incubated with sensitizing NPs, for example, AuNPs. Then the cells monolayer is exposed to the laser irradiation, thus resulting in photothermal effects of NPs, leading to a local increase in the membrane permeability. The most common photothermal effects are heating to a critical temperature or the formation of cavitation nano- and microbubbles due to the rapid evaporation of water surrounding NPs. The photosensibilized laser pulse by NP subsequently begins a rapid (10–1000 ns) expansion and collapse of cavitation bubbles, thus generating a localized mechanical force that partially destroys the cell membrane.[158] In recent few years, these effects have attracted particular attention of researchers, since the bubble generation is possible using less expensive pulsed ns lasers.[158,159] Lukianova-Hleb *et al.* used Au nanospheres and nanoshells as sensitizing NPs under the action of pulsed laser light (70 ps) to deliver FITC-dextran to CD3-positive Jurkat cells.[160] Xiong *et al.* demonstrated efficient (over 90%) delivery of labeled dextrans of different molecular weights to several cell lines using 70 nm NS and 7 ns laser.[161] Then the same group used this system to deliver labels to individual neurons, which allowed detailed study of their morphology.[162]

Cell optoporation systems using plasmon NPs that serve as sensibilizators of laser irradiation, called plasmon-induced optoporation, are demonstrating high efficacy in a wide range of cargo molecules sizes, maintained good cell viability, high

throughput (up to ≈100,000 cells/s), and compatibility with adherent and suspension cell cultures. It is notable that the possibility of integrating the laser sources systems with light (direct or confocal) microscopy opens up new opportunities for research in the field of intracellular biospecific labeling and targeting. However, the number of limitations restricts the transfer of current technologies to the clinical applications, one of which is associated with the cargo molecules size cutoff: a sufficient decrease in the delivery efficiency was shown for larger than 500 kDa molecules,[163] which is presumably related to a slower diffusion through the newly formed membrane disruptions. Another problem is the fragmentation of AuNPs due to the photomodification under the laser exposure.[164] The fragmentation phenomenon raises some concerns when applied to cell systems *in vivo*, since very small AuNPs can interact with DNA in cells, thereby increasing the likelihood of genotoxicity.[165,166] It was shown that particle fragmentation can be minimized by using off-resonant NPs with a fs pulsed laser[167,168] or by replacing the AuNP with more photostable materials, for example, graphene-based materials. Unfortunately, the fs lasers are extremely expensive, and graphene QDs[169] are significantly inferior to AuNPs in terms of photosensitizing characteristics and biocompatibility. Figure 6 depicts few recently developed AuNP-mediated optoporation systems, which in our opinion possess advantageous features and have potential upcoming perspectives.

3.3.2. *2D assembled plasmonic nanoplatforms for cell optoporation*

An alternative approach to eliminate the negative effects on cells in plasmon-induced optoporation systems is to replace the suspension of NPs with special nanosubstrates with similar NPs photothermal properties (Fig. 6(a)), which are simultaneously substrates for cell cultivation.[176] The implementation of such systems is as follows: laser irradiation causes local damage to the membranes of cells in the immediate vicinity by photothermal elements, ensuring the passage of nonpenetrating agents into the intracellular space.[173] One of the striking examples of such technologies is a biophotonic laser-assisted surgery tool (BLAST), which consists of a SiO_2 microparticles array coated with thin Ti films with the crescent shape.[177] One of the putative mechanisms for the formation of membrane holes (referred as "pores" in some issues) is the rupture of microcavitation bubbles, which facilitate efficient delivery (up to 78% of calcein-positive cells) while maintaining high viability (up to 87%).[178] Another example is the optoporation system using a continuous-wave (CW) laser with a wavelength of 808 nm and AuNPs layers (Fig. 6(c)), or magnetic iron oxide NPs.[179] When cells grown on pyramidal nanostructures (Fig. 6(e)) with a gold coating were exposed to a pulsed ns laser, a high delivery efficiency of a wide range of labeled dextrans was observed.[172] In combination with microfluidics, platforms with an array of gold nanotubes were fabricated for spatial-temporal and quantitative control of intracellular delivery.[180] Holes in cell membranes are formed by hot electrons after laser irradiation (1064 nm, 8 ps) with subsequent injection of PI into the microfluidic channel. Table 2 summarizes the recent data on the plasmonic assisted-optoporation systems.

Thus, platforms based on assembled NPs have significant advantages over systems based on suspension NPs, since their use completely excludes the internalization of NPs in the cells and all related questions. This aspect is especially attractive for potential *in vivo* applications. Another advantage is the possibility to use the CW lasers, as they are rather cheap than the pulsed laser suppliers. On the other hand, specialized substrates should be manufactured using special template microtechnologies,[177] which have poor scale-up ability, and noncompatible with suspended cells. Up until now, the *in vivo* investigations on NP-mediated intracellular delivery are rather scarce. The main reason is due to the limited tissue penetration of light, which limits the applicability, although NIR responsive photothermal NPs offer promising opportunities in this regard. Thus, it will be needed to directly address the photothermal NPs specifically to the host cells, apart from the effector molecules that should reach the same target site as well. Targeting of NPs and molecular drugs is extensively studied in the field of nanomedicine-mediated drug delivery and findings from that area may prove to be useful for translating NP-mediated transfection to *in vivo* applications as well. The most feasible application areas seem to be the skin and dedicated parts in the eye, especially since laser technologies are already approved for clinical surgery in ophthalmology, stomatology, and dermatology.

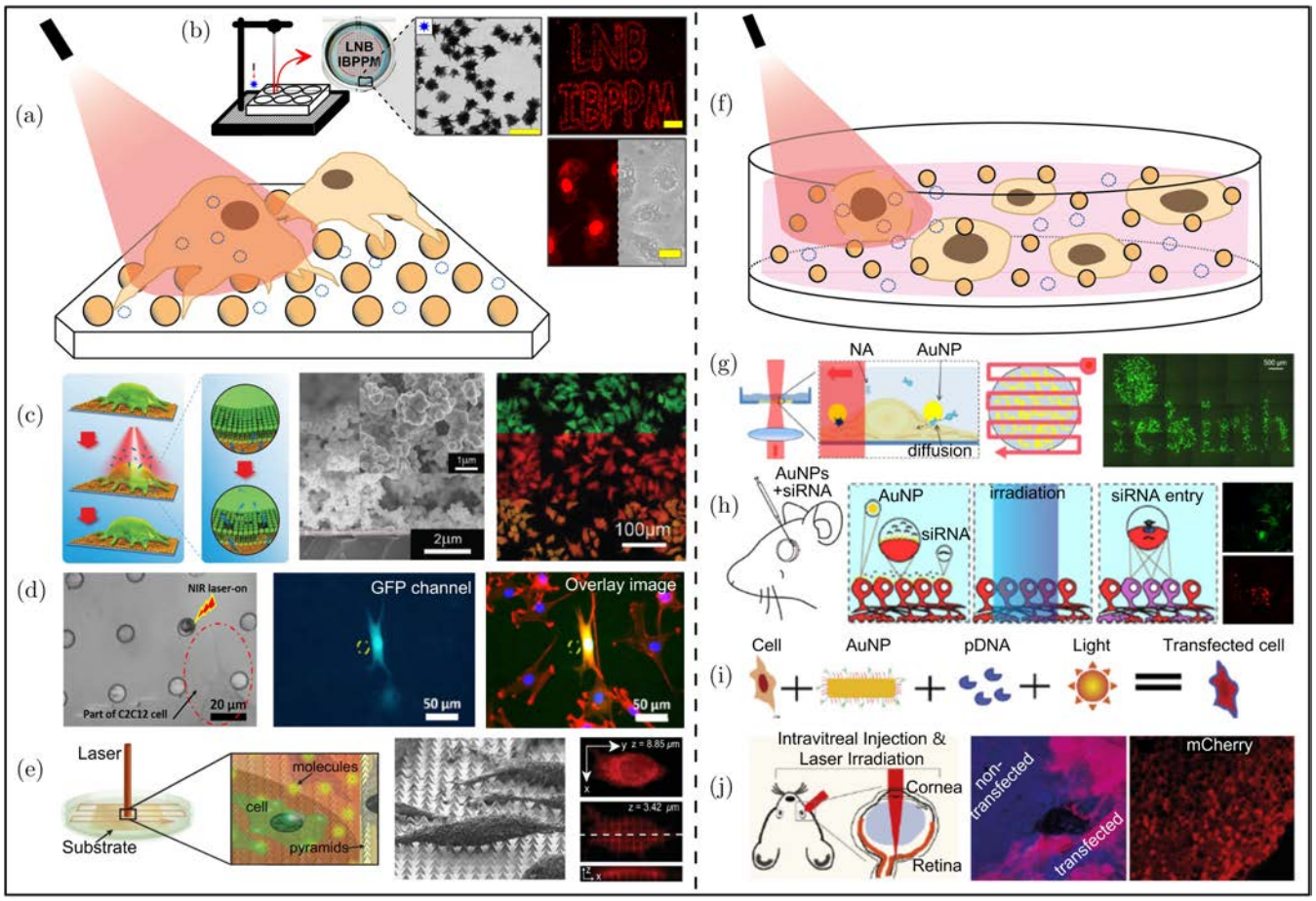

Fig. 6. Laser transfection systems based on photoactive plasmonic substrates (a)–(e) or with suspended AuNPs (f)–(j). Schematic representation of *in vitro* gene delivery to the cells adhered on the Au nanoarrays upon laser irradiation (a). Cell optoporation on culture plastic coated with Au nanostars layers. The fluorescent images show the optoporated HeLa cells with delivered PI molecules upon 1064-nm ns laser irradiation in 2D scanning mode (b). Reproduced with permissions from Ref. 170. Optoporation of the HeLa cells harvested on the AuNP surfaces for TRITC-dextran delivery via pores formation upon CW laser exposure (c). SEM images of AuNP surfaces prepared by chemical plating. Reproduced with permissions from Ref. Polymer-coated AuNPs deposited on a solid substrate (d): SEM image of the substrate, and fluorescence images of optoporated mouse fibroblast cells expressing GFP. Reproduced with permissions from Ref. 171. Lithography-assembled nanopyramids (e). Pulsed ns laser irradiation induce plasmonic nanoheating at the apex of each pyramid, cavitation bubbles formation that induce membrane poration. The SEM image shows the fixed HeLa cells on the substrate. Confocal images show Calcein red-orange delivered to the cells. Reproduced with permissions from Ref. 172. Principle of cell optoporation with AuNP suspension added to the cell medium (f). AuNP-labeled cells optoporation upon pulsed fs-laser irradiation in a scanning mode with focused beam (g) The representative fluorescence image of optoporated ZMTH3 cells merged from 24 single images. Reproduced from Ref. 173. Direct intravitreal injection of AuNPs, FITC, or siRNA into rat eye (h). FITC-dextran and Cy3-siRNA *in vivo* delivery to rat retinal cells by 800-nm fs laser irradiation in the presence of KV1.1-AuNPs. Reproduced with permissions from Ref. 174. The *in vivo* pDNA delivery to mouse retina cells upon CW NIR irradiation enhanced by functionalized Au NRs (i). The confocal images (j) of treated mice retina mCherry expression of (red) overlaid on nuclear stain DAPI (in blue). Reproduced from Ref. 175.

4. AuNP-Based Approaches for NA Detection

Specific and sensitive recognition of DNA in the biological samples is one of the major tasks of modern molecular diagnostics. The commercially available detection systems and reagents, on the basis of PCR, blotting, or similar techniques, are widely used for clinical trials,[189] in agriculture[190] environmental and food monitoring,[191] and other urgent goals. Nevertheless, conventional PCR-based tests are mostly unavailable in resource-limited settings, where sophisticated infrastructures, reliable electricity supplies, and trained operators are lacking. Point-of-care testing (POCT), on the other hand, permits rapid instrumentation-free

Table 2. Optoporation plasmonic assisted systems for targeted delivery in eukaryotic cells.

Laser parameters								
λ (nm)	Pulse duration	NP type	NP shape, size	Cargoes	Cell types	[a]Efficacy (%)	[b]Viability (%)	Year, Ref.
355	ns	—	—	pDNA	NRK	0.6	n.d.	1986, 181
800	fs	—	—	pDNA	CHO, PtK2	100	n.d.	2002, 182
532	ns	—	—	Labeled dextrans, pDNA	HeLa, NIH/3T3, 293T, HepG2,NTERA-2, PFSK-1, SU-DHL-4, CEM, 184A1, MO-2058	50	80	2006, 183
800	ps	—	—	PI	astrocyte rats, PC12	90	80	2008, 184
800	fs	Bessel light beam	n.d.	PI	CHO-K1, HL-60	26–34	n.d.	2012, 185
n.d.	n.d.	AuNP layers	Sphere, 133 nm	Low-range PEI, pDNA	HeLa, HUVECs, mEF,	94	40–80	2017, 157
820	ps	Au nanoshells	Sphere, 50 nm	pDNA	HN31, NOM 9	88	n.d.	2012, 159
561	ns	QD	10 nm	PI, labeled dextrans	*In vitro:* HeLa, C17.2, *In vivo:* INS-1E	80	80	2016, 161
561	ns	AuNPs	Sphere, 70 nm	Phalloidin	WT E18 C57Bl6	n.d.	n.d.	2018, 162
561	ns	Graphene QD	N.d.	Labeled dextrans	HeLa	50	70–80	2018, 186
532	ns	[2]BLAST	100-nm-thick titanium film, 3-μm hole on the SiO_2 membrane	Bacterial cells, labeled dextrans, enzymes	HeLa, NHDF, PB-MDM, RPTEC	40–50	90	2015, 177
1064	ns	SiO_2–Ti layers	Nanodisc, the cavities — 1 μ m, the pore — 800 nm	Calcein, labeled dextrans	HeLa CCL-2	78	87	2018, 178
808	∞	AuNP layers	Thin film	Labeled dextrans, pDNA	HeLa, mEF, HUVEC	80 (HeLa), 53 (mEF), 9 (HUVEC)	80 (HeLa), 95 (mEF), 90 (HUVEC)	2016, 187
808	∞	AuNP layers	Star, 80 nm	PI, labeled dextrans, pDNA	HeLa	98	95	2018, 170
808	∞	Pored magnetic iron oxide NPs	Sphere, 250 nm	Labeled dextrans, pDNA–PEI complexes	HeLa	67	92	2018, 179
1064	ns	Assembled Au pyramids	Pyramid 2.4 $\times$ 1.2μm	Calcein, labeled dextrans	HeLa CCL-2	95	98	2017, 188
1064	ns	Microfluidic Au nanotubes	Tube, 1.1 μm (height), 180 nm (diameter), 90 nm (inner nanochannel)	PI	NIH/3T3	95	n.d.	2015, 180

[a]The data is given in the percent of transfected cells counted by fluorescent images processing or by flow cytometry.
[b]The data is given in the percent and represents the results of live-dead staining and fluorescent bioimaging or cell respiratory assays.

analysis.[192] Two main criteria of POCT are the portability and versatility. To ensure the portability, the entire process, from sample preparation to signal amplification to readouts, should be without any additional instruments and/or alternating current power supplies. Many recent efforts have been dedicated to improve the portability of the signal amplification step.[193,194] Versatility is another great challenge. The ideal DNA POCT system should be compatible not only with diverse types of samples (such as saliva, urine, and blood) but also work with multiplex targets including pathogen-specific DNA sequences, gene mutations, single-nucleotide polymorphisms (SNPs), and allele genes.[195,196] Thus, AuNP-based technologies[197,198] can be considered as a promising alternative to the standard DNA-detection systems if they match mostly of the given criteria. As far as thousands of research studies and a broad list of reviews were recently published on current issue, in this section we provide a brief outline of the principal concepts for NA recognition by NP-based hybrid nanostructures. Specifically, the AuNP-based strategies can be divided into two groups: label and label-free (Fig. 7). The first one is related to the AuNP with covalently bonded sensing DNA, serving as probe. In a very simple explanation, the hybridization between the AuNP-labeled probe and complementary target DNA, in appropriate buffer conditions, induce the AuNP aggregation resulting in color change, modification of extinction and scattering spectra, and increased DLS average sizes (Figs. 7(a)–7(d)). These changes can be registered with rather good sensitivity using standard optical analyzers. Based on this strategy, implemented by Mirkin *et al.*,[22] plenty of assays were developed and investigated. The effects of salt, pH, proteins, and DNA base composition were discussed for controlling the conformation, density, and stability of DNA.[199] But still, there are several unsolved drawbacks. The synthetic procedure of DNA–AuNP covalent bonding is rather complicated, and practically nonsufficient with other types of AuNPs, this gain limits to multiplex analysis. This approach is rather expensive due to the usage of synthetic thiol-modified oligoDNA. In some cases, the assay has the pre-amplification step, which restricts an opportunity for equipment-free POCT format. Finally, the label concept "one probe for one target" is nonconvenient for search studies, with simultaneous big amount of different targets.

The other strategy relies on label-free assay format (Figs. 7(f)–7(i)), where AuNPs and all other components are interacting electrostatically due to the charges repulse, thus the system is quasi-static equilibrated. The electrostatic imbalance can be initiated by the probe–target hybridization, which in turn induces strong and irreversible AuNP aggregation in a target concentration-dependent manner, thus giving opportunity to sensitive and quantitative analysis. This simple concept was used in several studies,[196,202] including our recent approach[203] with CTAB-coated positively charged AuNPs (Fig. 7(h)). The beneficial features of such approaches are all related to label-free concept, so that you can easily change the target to be analyzed without any manipulations with AuNPs. This feature takes in advance to further commercialization as very simple, rapid, and cheap technology. But still it needs further investigations in order to optimize the reagents concentrations, AuNP parameters, and procedure conditions.

The two above described concepts for AuNP-based DNA detection were used in more complicated and smart approaches that compete for extremely high sensitivity and/or miniaturization[204] of the entire process. We just mention several examples of recently developed approaches[205–207] with heterogeneous-phase assay format (Fig. 8), in contrary to the described above homogeneous colorimetric tests, provided with AuNP colloid and other components in the liquid phase. Specifically, one of the assay components is chemically fixed on the special substrate (glass, paper, or other) thus forming the array of regularly deposited recognizing units. In combination with additional signal-enhancement step, for example Ag staining, the extremely LOD can be reached (up to zeptamolar concentration of target DNA,[206] Fig. 8(g)). It should be mentioned that further development of such array-based strategies is very promising and may give a good opportunity towards approved clinical usage.

5. NanoPCR — Polymerase Chain Reaction Enhanced with AuNPs

This section is devoted to the error-prone PCR and its improvement by AuNPs. The problem of poor specificity resulting in the appearance of smear bands along with specific band on the electrophoregram

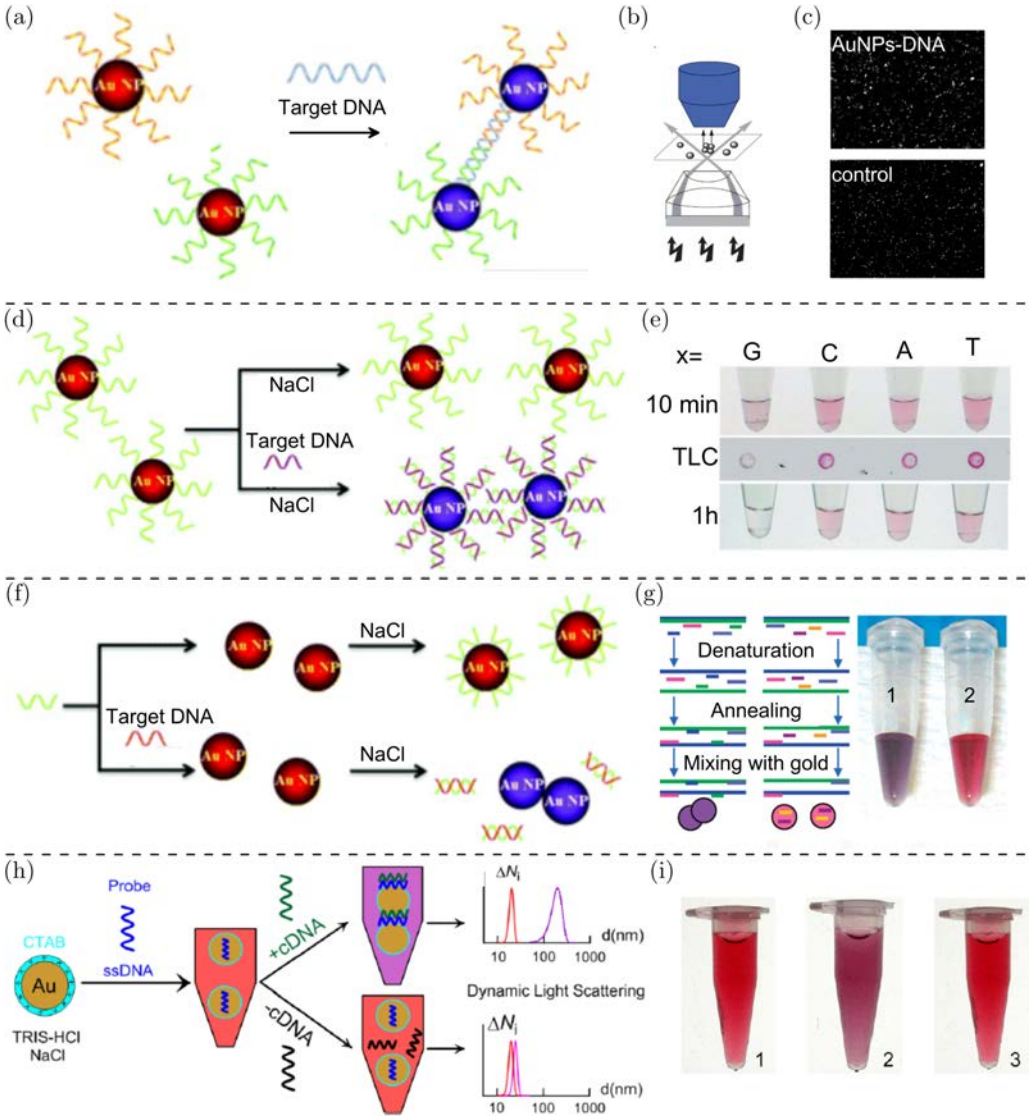

Fig. 7. AuNP-based strategies for homogeneous DNA detection. (a) Aggregation of AuNPs is induced by cross linking between two types of probeDNA–modified AuNPs hybridized with complementary target. The colorimetric response (b) and dark-field microscopy images (d) of nonaggregated (without target DNA, red) AuNP and aggregated (with target DNA, blue) colloid AuNPs. (c) Schematic illustration of the flash-lamp dark-field microscopy. Reproduced from Ref. 200. (d) Noncrosslinking aggregation-based strategy, visual (e) or semi-quantitative thin-liquid chromatography (TLC) detection of target DNA with single-nucleotide polymorphisms (f). The wild-type (X = G) and the mutants (others) can be discriminated by colors of the tubes (20 mL) or the spots on the TLC plate (2 mL). Reproduced from Ref. 201. (g) Colorimetric assay using electrostatically adsorbed DNA probes on AuNP surface. (h) Identification of PCR-amplified DNA sequences. The mixture of PCR product and probes is denatured and annealed below the melting temperature followed by addition of AuNP colloid. The long blue and green lines represent the amplified fragments (target), the pink and light blue medium bars represent the excess PCR primers. The short blue and green bars are complementary probes that bind, resulting in AuNP aggregation (purple color). The short purple and orange bars are noncomplementary probes that do not bind and adsorb to the AuNP, thus preventing aggregation (red color). Reproduced with permissions from Ref. 202. (h) CTAB-coated AuNPs for label-free oligoDNA discrimination with visual (i), UV-vis, and DLS detection. Reproduced with permissions from Ref. 203.

(EF) can be referred to inappropriate thermocycling conditions, nonoptimized ratio, and poor quality of the reagents used in the amplification mix and for NA extraction. Traditionally, the step-by-step optimization of the amplification mix, the thermocycler parameters, may help to improve the PCR efficacy and the yield of amplified product, but in several cases it remains unsolved. Latest generation of PCR machines can perform rapid heating-cooling cycles. The thermoelectric heating used in the PCR must be

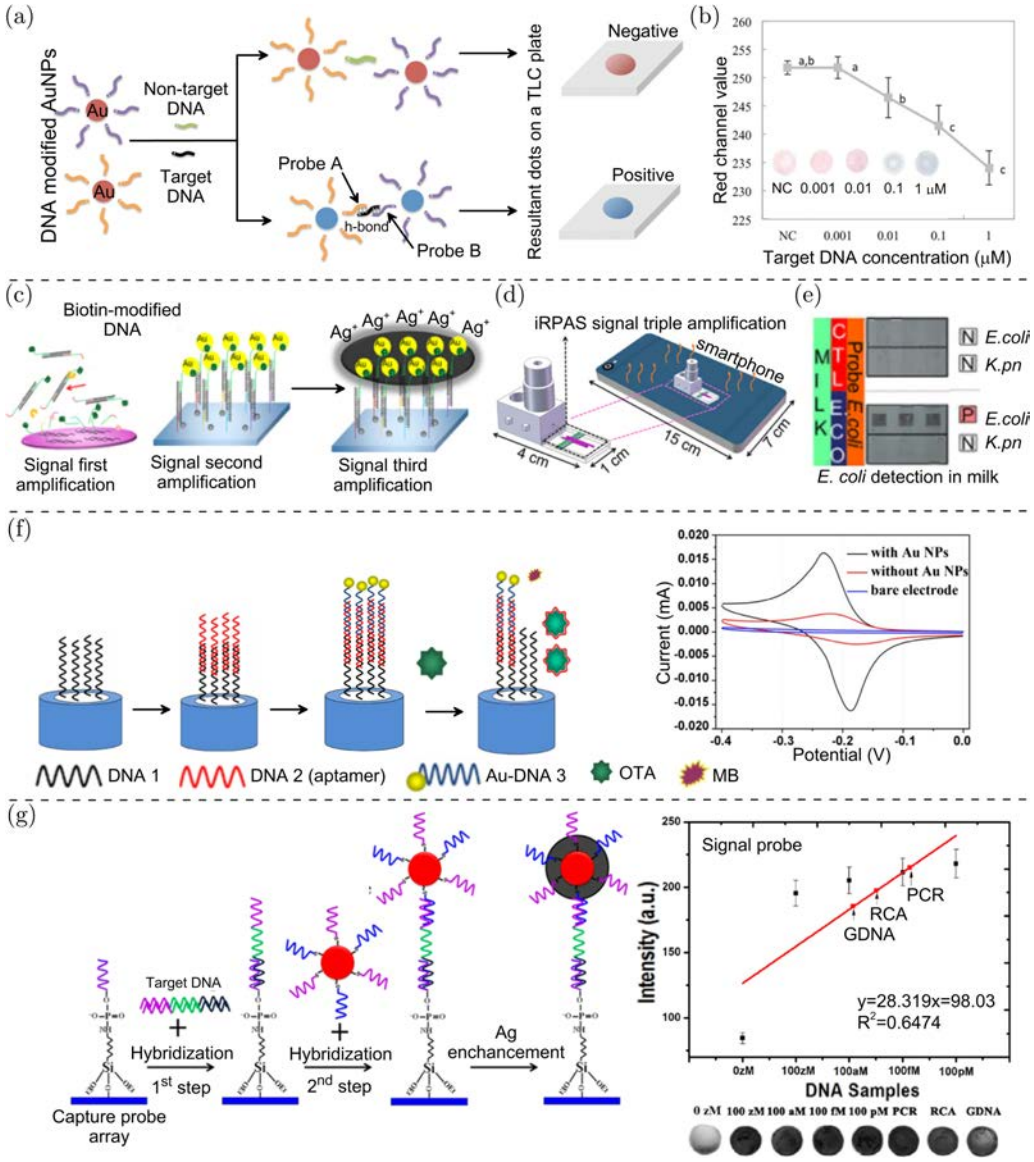

Fig. 8. AuNP-based heterogeneous sensors. (a) Cross-linking aggregation-based DNA assay with semi-quantitative TLC detector. (b) The linearity for the detection of target DNA was between 1 nM and 1 μM. Reproduced with permissions from Ref. 205. (c) Point-of-care kit for the entire DNA detection (POCKET). (d) Triple amplification combined on the isothermal recombinase polymerase amplification with a further Au biotin-streptavidin labeling and Ag enhancement. (e) Colorimetric readout with a smartphone. Reproduced from Ref. 204. (f) The aptamer-based sensor for the ochratoxin A (OTA) voltammetric detection. Reproduced with permissions from Ref. 206. (g) Sandwich-format scanometric assay with Ag enhancement for the detection of the amplified and genomic DNA. The arrayed capture oligoDNA is hybridized with the target DNA, then with the signal probe DNA conjugated with AuNPs followed by Ag staining. The LOD of scanometric detection of amplified DNA is about 100 zM. Reproduced with permissions from Ref. 207.

limited by the Peltier effect due to the powerful thermal flux and the relatively slow ratio of heating and cooling. To avoid this limitation, machines with an increased surface-to-volume ratio and a reduced volume of the reaction mixture have been developed, among them capillary PCR and PCR on microchips. The surface-to-volume ratio of the PCR chamber increased from 1.5 to 20 with the transition from conventional equipment to capillary PCR machines and to PCR equipment based on microarrays. This transition, however, made it possible to increase the PCR efficiency only 5–10 times.[208]

It is known that metal NPs with a decrease in their size have a higher thermal efficiency.[209] Specifically, the thermal conductivity can be increased by more than 20% when NPs are resuspended in

water.[210] In an aqueous solution, NPs can conduct heat and induce ultrafast thermal equilibration[211] in the microenvironment in 10–200 ps.[212] It is assumed that such an increase in thermal conductivity is due to a high surface-to-volume ratio,[213] the effect of particle clustering and electron pairing.

5.1. *The effect of AuNPs on conventional PCR with gel-EF detection*

Recently, it was shown that the addition of certain amount of NP in the amplification mixture can improve PCR performance.[214–220] Among them, AuNPs have attracted the greatest interest of researchers,[214–217] since the pioneer study, demonstrating the enhanced specificity of error-prone two-round PCR added to amplification mixture of nAuNPs.[214] Further, Li *et al.*[215] showed the similar effect of citrate AuNP on the efficiency of PCR. Then, Pan and co-workers[216] demonstrated the enhanced PCR selectivity assisted by AuNPs even for 7-cycle amplification. In addition, the certain amount of AuNP significantly enhanced the PCR efficiency when using common Taq-DNA polymerase[217] in complicated system. Several hypothetic mechanisms of AuNP-assisted PCR were proposed: (1) the single-stranded binding (SSB) protein-like mechanism[215] realized by electrostatic interactions between AuNPs and PCR components[221]; (2) the high surface-to-volume ratio of AuNPs and nonspecific adsorption of PCR components[218] on NPs surface; and (3) the thermal conductivity properties of AuNPs.[215,222] However, it is still unclear and debatable which of the suggested mechanisms is crucial for PCR outcome at typical amplification conditions. In this section, we provide a brief summary of the published data, including our recent mechanistic study.[223]

One of the questions is the role of AuNPs (the effect of material and surrounding media) on PCR outcome. No PCR improvement was observed when SiO_2 NPs were used instead of AuNPs[223] or when the dispersion medium from AuNP centrifugation was used instead of AuNP colloid,[214] thus clarifying the current role of AuNPs. The next question is the particle number concentration effect on PCR outcome. Li and co-workers[214] demonstrated that nonspecific smear bands gradually decreased within increased AuNP concentration from 0.2 nM to 0.8 nM. However, in the presence of an excess of AuNP amount (1 nM), the PCR was inhibited, which was registered in a reduced PCR yield. We have demonstrated the similar results on two various PCR model systems.[223] Thus, it was clarified that AuNPs act in a concentration-dependent manner.

Another group of questions are related to the effects of AuNPs on PCR components, such as template DNA, oligonucleotide primers, dNTPs, and polymerase; and the thermocycling profile. It is well-known that the annealing temperature of the oligoDNA primers affects greatly the PCR performance. The common way to improve the amplicon yield is to lower annealing temperature, while the specificity requires a higher annealing temperature. Thus, finding the optimal solution becomes rather difficult task, for example while using the "nested" PCR.[224] It was demonstrated[224] that in the presence of 0.4 nM AuNP, a single band corresponding to the specific amplicon can be obtained at a non-optimal annealing temperature of 40°C. The specific and high-yield amplification was achieved even at the annealing temperature of 25°C by using 0.6 nM AuNP. Thus, it was revealed that addition of AuNPs can contribute to the annealing temperature decrease, but there is no current explanation of this phenomenon to the date. The high temperature about 95°C used for DNA denaturation does provoke aggregation of citrate AuNPs or change their chemical properties, since citrate cannot react until the boiling point is reached. Thus, the rapid heat of the reaction mixture containing single AuNPs works as local PCR reactors by transferring the heat to PCR components thus enhancing the reaction kinetics. The melting point (T_m) is the temperature at which 50% of the dsDNA molecules can break down into individual ssDNA molecules. When T_m is reached, fast dissociation of duplexes occurs. The authors[225] revealed the lower limit of the melting temperature of DNA in PCR by adding AuNP. The melting temperature and the lowest temperature of DNA denaturation sample with presence of AuNP decreased by 1.5°C and 1°C, respectively, compared to real-time PCR without the addition of AuNP.

The next point is the effect of the DNA polymerase on PCR performance. It is known that the 1,6-Dithiothreitol (DTT) is commonly added to the PCR mixtures to preserve long-term activity of commercial Taq polymerase. The side effect of DTT is its negative effect on PCR specificity. It was

shown that AuNPs being added to the PCR mixture containing DTT were partially cross-linked by thiol groups of DTT via Au–S bonding, thus slightly decreased the positive effect of AuNPs on PCR outcome.[217] In another work, the possibility of suppressing the amplification of longer products and an increase in the yield of shorter amplicons was described.[226] The positive effect of AuNP coated with a monolayer of hexadecanethiol on PCR was observed when Taq and Tfl polymerases were used, but not Vent polymerase. It can be noted that the effects of NPs could be reversed with an increase in the concentration of polymerase or with the addition of BSA. Therefore, it was suggested that nanoparticles nonspecifically adsorb polymerase, thus effectively reducing its effective concentration.[226]

Another point that should be discussed is the AuNP size and surface ligand effects. Recently, it was demonstrated that depending on the size of the AuNP, inhibition of PCR occurs to a different degree.[227] This effect is based on the interaction of AuNP and iTaq polymerase. AuNPs have no direct effect on PCR efficiency at low particle concentration, while they inhibit PCR at concentrations above the threshold value. At the same concentration of particles, smaller AuNPs have a lower inhibitory effect on PCR than larger particles. According to the recent study,[227] the inhibitory effect is caused by the binding of iTaq polymerase and AuNP. BSA can also interact with AuNP and prevent the formation of polymerase binding sites on the particle surface. The inhibitory effect caused by AuNP can be partially removed by adding additional iTaq polymerase or BSA to the reaction mixture. In our recent work,[223] we explored the effects of variously charged AuNP capped with surface ligands, and estimated that the positively charged AuNPs have extremely high effect on PCR even at picomolar amounts, that is three-order lower than the working concentration of negatively charged citrate-capped AuNPs.

5.2. *The effect of AuNPs on real-time PCR*

The positive effect of AuNPs on the DNA degradation and SYBR Green fluorescence quenching upon their addition to a real-time PCR system was recently established.[228] The DNA degradation occurs due to the possible depurinization caused by elevated temperature. The change in the fluorescence signal caused by the addition of 2.09 nM AuNP was so small that it can be neglected when compared with the fluorescence signal of the amplified product. It was also shown that AuNPs form a complex only with native Taq polymerase and do not interact with recombinant rTaq polymerase. The improved real-time PCR with 13-nm AuNP[229] was applied for the detection of Japanese encephalitis virus DNA, isolated from clinical samples or from the culture. Based on the effect of increasing the thermal conductivity of the system with the addition of AuNPs, an original approach for real-time PCR using AuNRs[230] have been developed. The essence of the method consists in heating of the particles with an 808-nm IR laser, thus, improving the quality of DNA isolation from, after which real-time PCR is performed without removing the AuNRs from the system. It was shown that the PCR efficiency depends on the axial ratio (AR) of NRs, and reaches a maximum value at AR = 3 (compared to rods with AR = 15 and spherical particles).

To finalize the above discussion, it should be mentioned that rather simple modification in PCR system by adding the AuNPs can greatly improve its performance. We believe that nanoPCR can be implemented in the real clinical and laboratory practice, and will be helpful at the initial steps of newly developed PCR-based systems, as a one-step alternative to standard approaches optimizing the reagents and profile conditions. However, the current entire mechanisms underlying the described phenomenon still remain unclear due to the difficulty of providing model experiments and simulations for such multi-parameter system and need further investigations.

6. Concluding Remarks

We have briefly summarized the recent trends in engineering functional DNA-based plasmonic systems for multiple biomedical applications. With the rapid development of nanoparticles with desired optical, magnetic, and electronic properties, a variety of DNA–nanoparticle hybrids have been explored and designed for point-of-care diagnostics and targeted gene delivery. In laboratory settings, Au nanoparticle-based carriers have demonstrated good capability and efficacy as nonviral vectors for gene therapy. However, many circumstances remain to be explored before using good performance in cells or animal models for clinical use in patients.

More research is needed to better understand the determinants of *in vivo* performance. In particular, it remains unclear how the geometry of nanoparticles and surface modifications affect the pharmacokinetic bioavailability. The current mechanisms of interactions between cell surfaces, nanoparticles, and cargo molecules upon the laser irradiation, underlying the plasmonic-induced optoporation are needed to be further investigated. The challenges of nanoparticle-based detection systems are related to better optimization of the assay components for better performance, applicability, and versatility in order to develop universal platform for multiplex detection with simple, rapid, and cheap readout. We believe that further investigations are strongly needed to overcome these bottlenecks with regard to translate the plasmonic nanoparticles-mediated systems in the next generation biomedicine.

Conflicts of Interest

The authors declare that there are no conflicts of interest relevant to this paper.

Acknowledgments

The work by P.T.E. was supported by the Saratov State Medical University according to the research project No SSMU-2021-001. The part of the work (observation of SERS-based strategies) was supported by a grant from the Russian Science Foundation no. 18-14-00016-II.

References

1. X. Bai, Y. Wang, Z. Song, Y. Feng, Y. Chen, D. Zhang, L. Feng, "The basic properties of gold nanoparticles and their applications in tumor diagnosis and treatment," *Int. J. Mol. Sci.* **21**, 2480 (2020).
2. G. Go, C.-S. Lee, Y. M. Yoon, J. H. Lim, T. H. Kim, S. H. Lee, "PrP^C aptamer conjugated–gold nanoparticles for targeted delivery of doxorubicin to colorectal cancer cells," *Int. J. Mol. Sci.* **22**(4), 1976 (2021).
3. K. Saravanakumar, A. Sathiyaseelan, A. V. A. Mariadoss, X. Hu, K. Venkatachalam, M.-H. Wang, "Nucleolin targeted delivery of aptamer tagged *Trichoderma* derived crude protein coated gold nanoparticles for improved cytotoxicity in cancer cells," *Proc. Biochem.* **102**, 325–332 (2021).
4. D. Ferreira, D. Fontinha, C. Martins, D. Pires, A. R. Fernandes, P. V. Baptista, "Gold nanoparticles for vectorization of nucleic acids for cancer therapeutics," *Molecules* **25**, 3489 (2020).
5. M. Kheiro llahpour, M. Mehrabi, N. M. Dounighi, M. Mohammadi, A. Masoudi, "Nanoparticles and vaccine development. Pharmaceutical nanotechnology," *Pharma. Nanotechnol.* **8**(1), 6–21 (2020).
6. K. Saha, S. S. Agasti, C. Kim, X. Li, V. M. Rotello, "Gold nanoparticles in chemical and biological sensing," *Chem. Rev.* **112**(5), 2739–2779 (2012).
7. E. Ferrari, M. Soloviev, *Nanoparticles in Biology and Medicine Methods and Protocols*, Springer Science+Business Media Series, New York (2020).
8. Q. Guo, F. Hu, X. Yang, J. Yang, S. Yang, X. Chen, F. Wu, S. D. Minteer "*In-situ* and controllable synthesis of graphene-gold nanoparticles/molecularly imprinted polymers composite modified electrode for sensitive and selective rutin detection," *Microchem. J.* **158**, 105254 (2020).
9. T. Yang, Z. Luo, Y. Tian, C. Qian, Y. Duan, "Design strategies of AuNPs-based Nucleic Acid colorimetric biosensors," *Trends Anal. Chem.* **124**, 115795 (2020).
10. J. Simon, S. Udayan, E. S. Bindiy, S. G. Bhat, V. P. N. Nampoori, M. Kailasnath, "Optical characterization and tunable antibacterial properties of gold nanoparticles with common proteins," *Anal. Biochem.* **612**, 113975 (2021).
11. A. Ahmad, H. Liang, S. Ali, Q. Abbas, A. Farid, A. Ali, M. Iqbal, I. A. Khan, L. Pan, A. Abbas, Z. Farooq, "Cheap, reliable, reusable, thermally and chemically stable fluorinated hexagonal boron nitride nanosheets coated Au nanoparticles substrate for surface enhanced Raman spectroscopy," *Sens. Actuators B Chem.* **304**, 127394 (2020).
12. M. S. Kang, S. Y. Lee, K. S. Kim, D.-W. Han, "State of the art biocompatible gold nanoparticles for cancer theragnosis," *Pharmaceutics* **12**(8), 701 (2020).
13. L. Zhang, Y. Mazouzi, M. Salmain, B. Liedberg, S. Boujday, "Antibody-gold nanoparticle bioconjugates for biosensors: Synthesis, characterization and selected applications," *Biosens. Bioelectron.* **165**, 112370 (2020).
14. X. Tao, X. Wang, B. Liu, J. Liu, "Conjugation of antibodies and aptamers on nanozymes for developing biosensors," *Biosens. Bioelectron.* **168**, 112537 (2020).
15. M.-T. Chiang, H.-L. Wang, T.-Y. Han, Y.-K. Hsieh, J. Wang, D.-H. Tsai, "Assembly and detachment of hyaluronic acid on a protein-conjugated gold nanoparticle," *Langmuir* **36**(48), 14782–14792 (2020).
16. B. Tan, F. Baycan, "A new donor-acceptor conjugated polymer-gold nanoparticles biocomposite

materials for enzymatic determination of glucose," *Polymer* **210**, 123066 (2020).
17. Y. Gao, Y. Liu, R. Yan, J. Zhou, H. Dong, X. Hua, P. Wang, "Bifunctional peptide-conjugated gold nanoparticles for precise and efficient nucleus-targeting bioimaging in live cells," *Anal. Chem.* **92** (19), 13595–13603 (2020).
18. Z. Wang, J. Dong, Q. Zhao, Y. Ying, L. Zhang, J. Zou, S. Zhao, J. Wang, Y. Zhao, S. Jiang, "Gold nanoparticle mediated delivery of paclitaxel and nucleic acids for cancer therapy (Review)," *Mol. Med. Rep.* **22**(6), 4475–4484 (2020).
19. E. Aali, A. S. Rad, M. Esfahanian, "Computational investigation of the strategy of DNA/RNA stabilization through the study of the conjugation of an oligonucleotide with silver and gold nanoparticles," *Appl. Organomet. Chem.* **34**(8), e5690 (2020).
20. Y. Hao, Y. Li, L. Song, Z. Deng, "Flash synthesis of spherical nucleic acids with record DNA density," *Am. Chem. Soc.* **143**(8), 3065–3069 (2021).
21. O. Mukama, J. Wu, Z. Li, Q. Liang, Z. Yi, X. Lu, Y. Liu, Y. Liu, M. Hussain, G. G. Makafe, J. Liu, N. Xu, L. Zeng, "An ultrasensitive and specific point-of-care CRISPR/Cas12 based lateral flow biosensor for the rapid detection of nucleic acids," *Biosens. Bioelectron.* **159**, 112143 (2020).
22. C. Mirkin, R. Letsinger, R. Mucic, R. C. Mucic, J. J. Storhoff, "A DNA-based method for rationally assembling nanoparticles into macroscopic materials," *Nature* **382**, 607–609 (1996).
23. L. Fang, D. Liu, Y. Wang, Y. Li, L. Song, M. Gong, Y. Li, Z. Deng, "Nanosecond-laser-based charge transfer plasmon engineering of solution-assembled nanodimers," *Nano Lett.* **18**, 7014–7020 (2018).
24. N. Liu, T. Liedl, "DNA-assembled advanced plasmonic architectures," *Chem. Rev.* **118**, 3032–3053 (2018).
25. W. Zhou, Q. Li, H. Liu, J. Yang, D. Liu, "Building electromagnetic hot spots in living cells via target-triggered nanoparticle dimerization," *ACS Nano* **11**, 3532–3541 (2017).
26. J. Liu, Y. A. Lu, "Colorimetric lead biosensor using DNAzyme-directed assembly of gold nanoparticles," *J. Am. Chem. Soc.* **125**, 6642–6643 (2003).
27. S. M. Taghdisi, N. M. Danesh, M. Ramezani, A. S. Emrani, K. Abnous, "Novel colorimetric aptasensor for zearalenone detection based on nontarget-induced aptamer walker, gold nanoparticles, and exonuclease-assisted recycling amplification," *ACS Appl. Mater. Interfaces* **10**, 12504–12509 (2018).
28. Z. Long, M. Liu, L. Mao, G. Zeng, Q. Huang, H. Huang, F. Deng, Y. Wan, X. Zhang, Y. Wei, "One-step synthesis, self-assembly and bioimaging applications of adenosine triphosphate containing amphiphilies with aggregation-induced emission feature," *Mater. Sci. Eng. C Mater. Biol. Appl.* **73**, 252–256 (2017).
29. W. Nie, Q. Wang, L. Zou, Y. Zheng, X. Liu, X. Yang, K. Wang, "Low-fouling surface plasmon resonance sensor for highly sensitive detection of microRNA in a complex matrix based on the DNA tetrahedron," *Anal. Chem.* **90**, 12584–12591 (2018).
30. X. Zhou, C. T. Yang, Q. Xu, Z. Lou, Z. Xu, B. Thierry, N. Gu, "Gold nanoparticle probe-assisted antigen-counting chip using SEM," *ACS Appl. Mater. Interfaces* **11**, 6769–6776 (2019).
31. L. Feng, L. Wu, F. Xing, L. Hu, J. Ren, X. Qu, "Novel electrochemiluminescence of silver nanoclusters fabricated on triplex DNA scaffolds for label-free detection of biothiols," *Biosens. Bioelectron.* **98**, 378–385 (2017).
32. J. Wang, J. Huang, K. Quan, J. Li, Y. Wu, Q. Wei, X. Yang, K. Wang, "Hairpin-fuelled catalytic nanobeacons for amplified microRNA imaging in live cells," *Chem. Commun.* **54**, 10336–10339 (2018).
33. C. Zhang, J. P. Kim, M. Creer, J. Yang, Z. Liu, "A smartphone-based chloridometer for point-of-care diagnostics of cystic fibrosis," *Biosens. Bioelectron.* **97**, 164–168 (2017).
34. M. E. Kyriazi, D. Giust, A. H. El-Sagheer, P. M. Lackie, O. L. Muskens, T. Brown, A. G. Kanaras, "Multiplexed mRNA Sensing and combinatorial-targeted drug delivery using DNA-gold nanoparticle dimers," *ACS Nano* **12**, 3333–3340 (2018).
35. P. Vilela, A. Heuer-Jungemann, A. El-Sagheer, T. Brown, O. L. Muskens, N. Smyth, A. G. Kanaras, "Sensing of vimentin mRNA in 2D and 3D models of wounded skin using DNA coated gold nanoparticles," *Small* **14**, e1703489 (2018).
36. C. H. Choi, L. Hao, S. P. Narayan, E. Auyeung, C. A. Mirkin, "Mechanism for the endocytosis of spherical nucleic acid nanoparticle conjugates," *Proc. Natl. Acad. Sci. U. S. A.* **110**, 7625–7630 (2013).
37. D. A. Giljohann, D. S. Seferos, P. C. Patel, J. E. Millstone, N. L. Rosi, C. A. Mirkin, "oligonucleotide loading determines cellular uptake of DNA-Modified gold nanoparticles," *Nano Lett.* **7**, 3818–3821 (2007).
38. Y. Yang, S. Zhong, K. Wang, J. Huang, "Gold nanoparticle based fluorescent oligonucleotide probes for imaging and therapy in living systems," *Analyst* **144**, 1052–1072 (2019).
39. U. Heinemann, Y. Roske, "Symmetry in nucleic-acid double helices," *Symmetry* **12**(5), 737 (2020).
40. H. Sato, S. Das, R. H. Singer, M. Vera, "Imaging of DNA and RNA in living eukaryotic cells to reveal spatiotemporal dynamics of gene expression," *Annu. Rev. Biochem.* **89**, 159–187 (2020).

41. J. K. Kulski, Next-generation sequencing — An overview of the history, tools, and "omic" application, *Next Generation Sequencing - Advances, Applications and Challenges*, Chap. 1, J. K. Kulski, Ed., pp. 3–60, InTech (2016).
42. R. A. Hughes, A. D. Ellington, "Synthetic DNA synthesis and assembly: putting the synthetic in synthetic biology," *Cold Spring Harb. Perspect. Biol.* **9**(1), a023812 (2017).
43. O. I. Wilner, I. Willner, "Functionalized DNA nanostructures," *Chem. Rev.* **112**(4), 2528–2556 (2012).
44. C. Kimna, O. Lieleg, "Molecular micromanagement: DNA nanotechnology establishes spatiotemporal control for precision medicine," *Biophys. Rev.* **1**, 011305 (2020).
45. F. Xu, Q. Xia, P. Wang, "Rationally designed DNA nanostructures for drug delivery," *Front. Chem.* **8**, 751 (2020).
46. X. Yan, S. Huang, Y. Wang, Y. Tang, Y. Tian, "Bottom-up self-assembly based on DNA nanotechnology," *Nanomaterials* **10**(10), 2047 (2020).
47. M. Hawner, C. Ducho, "Cellular targeting of oligonucleotides by conjugation with small molecules," *Molecules* **25**(24), 5963 (2020).
48. J. Bruno, "A review of therapeutic aptamer conjugates with emphasis on new approaches," *Pharmaceuticals* **6**(3), 340–357 (2013).
49. N. Rabiee, S. Ahmadi, Z. Arab, M. Bagherzadeh, M. Safarkhani, B. Nasseri, M. Rabiee, M. Tahriri, T. J. Webster, L. Tayebi, "Aptamer hybrid nanocomplexes as targeting components for antibiotic/gene delivery systems and diagnostics: A review," *Int. J. Nanomed.* **15**, 4237–4256 (2020).
50. H. Ling, F. Xiaoyi, K. G. Y. Yao, M. Hongmin, K. Guoliang, Z. Xiaobing, "DNAzyme-gold nanoparticle-based probes for biosensing and bioimaging," *J. Mater. Chem. B* **8**, 9449–9465 (2020).
51. S. Siddiquee, K. Rovina, A. Azriah, "A review of peptide nucleic acid," *Adv. Tech. Biol. Med.* **3**(2), 131 (2015).
52. S. Ochoa, V. T. Milam, "Modified nucleic acids: expanding the capabilities of functional oligonucleotides," *Molecules* **25**, 4659 (2020).
53. X. Li, K. Feng, L. Li, L. Yang, X. Pan, H. S. Yazd, C. Cui, J. Li, L. Moroz, Y. Sun, B. Wang, X. Li, T. Huang, W. Tan, "Lipid–oligonucleotide conjugates for bioapplications," *Natl. Sci. Rev.* **7**, 1933–1953 (2020).
54. N. Dias, C. A. Stein, "Antisense oligonucleotides: Basic concepts and mechanisms," *Mol. Cancer Ther.* **1**, 347–355 (2002).
55. A. Kilanowska, S. Studzińska, "*In vivo* and *in vitro* studies of antisense oligonucleotides – A review," *RSC Adv.* **10**, 34501–34516 (2020).
56. S. Volpi, U. Cancelli, M. Neri, R. Corradini, "Multifunctional delivery systems for peptide nucleic acids," *Pharmaceuticals.* **14**(1), 14 (2021).
57. Y. Zhao, C. Xu, "DNA based plasmonic heterogeneous nanostructures: Building, optical responses, and bioapplications," *Adv. Mat.* **32**(41), 1907880 (2020).
58. L. A. Dykman, N. G. Khlebtsov, "Methods for chemical synthesis of colloidal gold," *Russ. Chem. Rev.* **88**(3), 229–247 (2019).
59. X.-Y. Liu, C.-B. Zhou, C. Fang, "Nanomaterial-involved neural stem cell research: Disease treatment, cell labeling, and growth regulation," *Biomed. Pharmacother.* **107**, 583–597 (2018).
60. Q. Jiang, S. Zhao, J. Liu, L. Song, Z.-G. Wang, B. Ding, "Rationally designed DNA-based nanocarriers," *Adv. Drug Deliv. Rev.* **147**, 2–21 (2019).
61. V. Raji, K. Pal, T. Zaheer, N. Kalarikkal, S. Thomas, F. G. de Souza, A. Si, "Gold nanoparticles against respiratory diseases: oncogenic and viral pathogens review," *Ther. Deliv.* **11**(8), 521–534 (2020).
62. N. H. Abd Ellah, S. F. Gad, K. Muhammad, G. E. Batiha, H. F. Hetta, "Nanomedicine as a promising approach for diagnosis, treatment and prophylaxis against COVID-19," *Nanomedicine* **15**, 21 (2020).
63. L. Yang, H. Sun, X. Wang, W. Yao, W. Zhang, L. Jiang, "An aptamer based aggregation assay for the neonicotinoid insecticide acetamiprid using fluorescent upconversion nanoparticles and DNA functionalized gold nanoparticles," *Microchim. Acta* **186**, 308 (2019).
64. Z. Hou, Z. Wang, R. Liu, H. Li, Z. Zhang, T. Su, J. Yang, H. Liu, "The effect of phospho-peptide on the stability of gold nanoparticles and drug delivery," *J. Nanobiotechnol.* **17**, 88 (2019).
65. A. Gupta, D. F. Moyano, A. Parnsubsakul, A. Papadopoulos, L.-S. Wang, R. F. Landis, R. Das, V. M. Rotello, "Ultrastable and biofunctionalizable gold nanoparticles," *ACS Appl. Mater. Interfaces* **8**(22), 14096–14101 (2016).
66. X.-Y. Li, F.-Y. Feng, Z.-T. Wu, Y.-Z. Liu, X.-D. Zhou, J.-M. Hu, "High stability of gold nanoparticles towards DNA modification and efficient hybridization via a surfactant-free peptide route," *Chem. Commun.* **53**, 11909–11912 (2017).
67. S. S. Hinman, K. S. M. Keating, Q. Cheng, "DNA linkers and diluents for ultrastable gold nanoparticle bioconjugates in multiplexed assay development," *Anal. Chem.* **89**, 4272–4279 (2017).
68. J. Deka, R. Měch, L. Ianeselli, H. Amenitsch, F. Cacho-Nerin, P. Parisse, L. Casalis, "Surface passivation improves the synthesis of highly stable and specific DNA-functionalized gold nanoparticles

with variable DNA density," *ACS Appl. Mater. Interfaces* **7**(12), 7033–7040 (2015).
69. J. H. Heo, K.-I. Kim, H. H. Cho, J. W. Lee, B. S. Lee, S. Y. Yoon, K. J. Park, S. Lee, J. Kim, D. Whang, J. H. Lee, "Ultrastable-stealth large gold nanoparticles with DNA directed biological functionality," *Langmuir* **31**(51), 13773–13782 (2015).
70. J. Li, B. Zhu, Y. Xiujie, Y. Zhang, Z. Zhu, S. Tu, S. Jia, R. Liu, H. Kang, C. J. Yang, "A synergetic approach for simple and rapid conjugation of gold nanoparticles with oligonucleotides," *ACS Appl. Mater. Interfaces* **6**, 16800–16807 (2014).
71. J. H. Heo, H. H. Cho, J. H. Lee, "Surfactant-free nanoparticle–DNA complexes with ultrahigh stability against salt for environmental and biological sensing," *Analyst* **139**, 5936–5944 (2014).
72. J. Gao, X. Huang, H. Liu, F. Zan, J. Ren, "Colloidal Stability of gold nanoparticles modified with thiol compounds: Bioconjugation and application in cancer cell imaging," *Langmuir* **28**(9), 4464–4471 (2012).
73. S. J. Hurst, A. K. R. Lytton-Jean, C. A. Mirkin, "Maximizing DNA loading on a range of gold nanoparticle sizes," *Anal. Chem.* **78**(24), 8313–8318 (2006).
74. X. Liu, G. Liao, L. Zou, Y. Zheng, X. Yang, Q. Wang, X. Geng, S. Li, Y. Liu, K. Wang, "Construction of bio/nanointerfaces: Stable gold nanoparticle bioconjugates in complex systems," *ACS Appl. Mater. Interfaces* **11**(43), 40817–40825 (2019).
75. J. H. Joo, J.-S. Lee, "Library approach for reliable synthesis and properties of DNA-gold nanorod conjugates," *Anal. Chem.* **85**, 6580–6586 (2013).
76. A. Wijaya, K. Hamad-Schifferli, "Ligand customization and DNA functionalization of gold nanorods via round-trip phase transfer ligand exchange," *Langmuir* **24**, 9966–9969 (2008).
77. C.-C. Chen, Y.-P. Lin, C.-W. Wang, H.-C. Tzeng, C.-H. Wu, Y.-C. Chen, C.-P. Chen, L.-C. Chen, Y.-C. Wu, "DNA-gold nanorod conjugates for remote control of localized gene expression by near infrared irradiation," *J. Am. Chem. Soc.* **128**, 3709–3715 (2006).
78. S. Pal, Z. Deng, H. Wang, S. Zou, Y. Liu, H. Yan, "DNA directed self-assembly of anisotropic plasmonic nanostructures," *J. Am. Chem. Soc.* **133**, 17606–17609 (2011).
79. D. Shi, C. Song, Q. Jiang, Z.-G. Wang, B. Ding, "A facile and efficient method to modify gold nanorods with thiolated DNA at a low pH value," *Chem. Commun.* **49**, 2533–2535 (2013).
80. U. Das, A. Sahoo, S. Haldar, S. Bhattacharya, S. S. Mandal, W. H. Gmeiner, S. Ghosh, "Secondary structure-dependent physicochemical interaction of oligonucleotides with gold nanorod and photothermal effect for future applications: a new insight," *ACS Omega* **3**(10), 14349–14360 (2018).
81. I. C. Pekcevik, L. C. H. Poon, M. C. P. Wang, B. D. Gates, "Tunable loading of single-stranded DNA on gold nanorods through the displacement of polyvinylpyrrolidone," *Anal. Chem.* **85**, 9960–9967 (2013).
82. J. D. Carter, T. H. LaBean, "Organization of inorganic nanomaterials via programmable DNA self-assembly and peptide molecular recognition," *ACS Nano* **5**, 2200–2205 (2011).
83. A. P. Alivisatos, K. P. Johnsson, X. Peng, T. E. Wilson, C. J. Loweth, M. P. Bruchez, P. G. Schultz, "Organization of 'nanocrystal molecules' using DNA," *Nature* **382**, 609–611 (1996).
84. E. Auyeung, T. I. N. G. Li, A. J. Senesi, A. L. Schmucker, B. C. Pals, M. O. de la Cruz, C. A. Mirkin, "DNA-mediated nanoparticle crystallization into Wulff polyhedral," *Nature* **505**, 73–77 (2014).
85. F. Lu, K. G. Yager, Y. Zhang, H. Xin, O. Gang, "Superlattices assembled through shape-induced directional binding," *Nat. Commun.* **6**, 6912 (2015).
86. J. E. Millstone, D. G. Georganopoulou, X. Xu, W. Wei, S. Li, C. A. Mirkin, "DNA-gold triangular nanoprism conjugates," *Small* **4**(12), 2176–2180 (2008).
87. J.-Y. Kim, J.-S. Lee, "Synthesis and thermodynamically controlled anisotropic assembly of DNA-Silver Nanoprism conjugates for diagnostic applications," *Chem. Mater.* **22**(24), 6684–6691 (2010).
88. H.-G. Park, J. H. Joo, H.-G. Kim, J.-S. Lee, "Shape-dependent reversible assembly properties of polyvalent DNA-silver nanocube conjugates," *J. Phys. Chem.* **116**(3), 2278–2284 (2011).
89. M. R. Jones, R. J. Macfarlane, B. Lee, J. Zhang, K. L. Young, A. J. Senesi, C. A. Mirkin, "DNA-nanoparticle superlattices formed from anisotropic building blocks," *Nat. Mater.* **9**, 913–917 (2010).
90. E. Dujardin, L.-B. Hsin, C. R. C. Wangb, S. Mann, "DNA-driven self-assembly of gold nanorods," *Chem. Commun.* **14**, 1264–1265 (2001).
91. E. Yasun, B. Gulbakan, I. Ocsoy, Q. Yuan, M. I. Shukoor, C. Li, W. Tan, "Enrichment and detection of rare proteins with aptamer-conjugated gold nanorods," *Anal. Chem.* **84**(14), 6008–6015 (2012).
92. C.-C. Chen, Y.-P. Lin, C.-W. Wang, H.-C. Tzeng, C.-H. Wu, Y.-C. Chen, C.-P. Chen, L.-C. Chen, Y.-C. Wu, "DNA-gold nanorod conjugates for remote control of localized gene expression by near infrared irradiation," *J. Am. Chem. Soc.* **128**(11), 3709–3715 (2006).
93. S. Pal, Z. Deng, H. Wang, S. Zou, Y. Liu, H. Yan, "DNA directed self-assembly of anisotropic

plasmonic nanostructures," *J. Am. Chem. Soc.* **133**(44), 17606–17609 (2011).
94. D. Shi, C. Song, Q. Jiang, Z.-G. Wanga, B. Ding, "A facile and efficient method to modify gold nanorods with thiolated DNA at a low pH value," *Chem. Commun.* **49**, 2533–2535 (2013).
95. S. Mann, "Life as a nanoscale phenomenon," *Angew. Chem. Int. Ed.* **47**(29), 5306–5320 (2008).
96. H. Lin, S. Lee, L. Sun, M. Spellings, M. Engel, S. C. Glotzer, "Clathrate colloidal crystals," *Science* **355**(6328), 931–935 (2017).
97. M. Loretan, I. Domljanovic, M. Lakatos, C. Rüegg, G. P. Acuna, "DNA origami as emerging technology for the engineering of fluorescent and plasmonic-based biosensors," *Materials* **13**(9), 2185 (2020).
98. F. F. Lu, T. Vo, Y. Zhang, A. Frenkel, K. G. Yager, S. Kumar, O. Gang, "Unusual packing of soft-shelled nanocubes," *Sci. Adv.* **5**(5), 2399 (2019).
99. S. Li, L. Xu, W. Ma, X. Wu, M. Sun, H. Kuang, L. Wang, N. A. Kotov, C. Xu, "Dual-mode ultrasensitive quantification of microRNA in living cells by chiroplasmonic nanopyramids self-assembled from gold and upconversion nanoparticles," *J. Am. Chem. Soc.* **138**, 306 (2016).
100. L. Xu, H. Kuang, C. Xu, W. Ma, L. Wang, N. A. Kotov, "Regiospecific plasmonic assemblies for *in situ* Raman spectroscopy in live cells," *J. Am. Chem. Soc.* **134**, 1699 (2012).
101. Y. Wang, B. Yan, L. Chen, "SERS Tags: Novel optical nanoprobes for bioanalysis," *Chem. Rev.* **113**(3), 1391–1428 (2013).
102. J. R. Lakowicz, Introduction to fluorescence, *Principles of Fluorescence Spectroscopy*, Chap. 1, J. R. Lakowicz, Ed., pp. 1–26, Springer, US, New York (2006).
103. J.-M. Nam, J.-W. Oh, H. Lee, Y. D. Suh, "Plasmonic nanogap-enhanced Raman scattering with nanoparticles," *Acc. Chem. Res.* **49**(12), 2746–2755 (2016).
104. N. G. Khlebtsov, L. Lin, B. N. Khlebtsov, J. Ye, "Gap-enhanced Raman tags: fabrication, optical properties, and theranostic applications," *Theranostics* **10**(5), 2067–2094 (2020).
105. D.-K. Lim, K.-S. Jeon, J.-H. Hwang, H. Kim, S. Kwon, Y. D. Shu, J.-M. Nam, "Highly uniform and reproducible surface-enhanced Raman scattering from DNA-tailorable nanoparticles with 1-nm interior gap," *Nat Nano* **6**, 452–460 (2011).
106. W. Kang, P. T. C. So, R. R. Dasari, D.-K. Lim, "High resolution live cell Raman imaging using subcellular organelle-targeting SERS-sensitive gold nanoparticles with highly narrow intra-nanogap," *Nano Lett.* **15**, 1766–1772 (2015).
107. J.-W. Oh, D.-K. Lim, G.-H. Kim, Y. D. Suh, J. Nam, "Thiolated DNA-based chemistry and control in the structure and optical properties of plasmonic nanoparticles with ultrasmall interior nanogap," *J. Am. Chem. Soc.* **136**, 14052–14059 (2014).
108. Y. Zhang, P. Yang, M. A. H. Muhammed, S. K. Alsaiari, B. Moosa, A. Almalik, A. Kumar, E. Ringe, N. M. Khashab, "Tunable and linker free nanogaps in core–shell plasmonic nanorods for selective and quantitative detection of circulating tumor cells by SERS," *ACS Appl. Mater. Interfaces* **9**(43), 37597–37605 (2017).
109. E. Yang, D. Li, P. Yin, Q. Xie, Y. Li, Q. Lin, Y. Duan, "A novel surface-enhanced Raman scattering (SERS) strategy for ultrasensitive detection of bacteria based on three-dimensional (3D) DNA walker," *Biosens. Bioelectron.* **172**, 112758 (2021).
110. J.-H. Lee, M. H. You, G.-H. Kim, J.-M. Nam, "Plasmonic nanosnowmen with a conductive junction as highly tunable nanoantenna structures and sensitive, quantitative and multiplexable surface-enhanced Raman scattering probes," *Nano Lett.* **14**(11), 6217–6225 (2014).
111. J.-W. Chen, X.-P. Liu, K.-J. Feng, Y. Liang, J.-H. Jiang, G.-L. Shen, R.-Q. Yu, "Detection of adenosine using surface-enhanced Raman scattering based on structure-switching signaling aptamer," *Biosens. Bioelectron.* **24**(1), 66–71 (2008).
112. J. Prinz, B. Schreiber, L. Olejko, J. Oertel, J. Rackwitz, A. Keller, I. Bald, "DNA origami substrates for highly sensitive surface-enhanced Raman scattering," *J. Phys. Chem. Lett.* **4**(23), 4140–4145 (2013).
113. L. Z. Chen, J. Chao, X. M. Qu, H. B. Zhang, D. Zhu, S. Su, A. Aldalbahi, L. H. Wang, H. Pei, "Probing cellular molecules with polyA-based engineered aptamer nanobeacon," *ACS Appl. Mater. Interfaces* **9**, 8014–8020 (2017).
114. D. S. Seferos, D. A. Giljohann, H. D. Hill, A. E. Prigodich, C. A. Mirkin, "Nano-flares: probes for transfection and mRNA detection in living cells," *J. Am. Chem. Soc.* **129**(50), 15477–15479 (2007).
115. P. W. Wu, K. V. Hwang, T. Lan, Y. Lu, "A DNAzyme-Gold nanoparticle probe for uranyl ion in living cells," *J. Am. Chem. Soc.* **135**, 5254–5257 (2013).
116. H.-Y. Yeh, M. V. Yates, A. Mulchandani, W. Chen, "Molecular beacon–quantum dot–Au nanoparticle hybrid nanoprobes for visualizing virus replication in living cells," *Chem. Commun.* **46**, 3914–3916 (2010).
117. W. Liu, H. Wei, Z. Lin, S. Mao, J.-M. Lin, "Rare cell chemiluminescence detection based on aptamer-specific capture in microfluidic channels," *Biosens. Bioelectron.* **28**(1), 438–442 (2011).

118. C. Hu, J. Shen, J. Yan, J. Zhong, W. Qin, R. Liu, A. Aldalbahi, X. Zuo, S. Song, C. Fanc, D. He, "Highly narrow nanogap-containing Au@Au core-shell SERS nanoparticles: Size-dependent Raman enhancement and applications in cancer cell imaging," *Nanocale* **8**, 2090–2096 (2016).
119. J. W. Kang, P. T. C. So, R. R. Dasari, D.-K. Lim, "High resolution live cell Raman imaging using subcellular organelle-targeting SERS-sensitive gold nanoparticles with highly narrow intra-nanogap," *Nano Lett.* **15**(3), 1766–1772 (2015).
120. S. Pal1, A. Ray, C. Andreou, Y. Zhou, T. Rakshit, M. Wlodarczyk, M. Maeda, R. Toledo-Crow, N. Berisha, J. Yang, H.-T. Hsu, A. Oseledchyk, J. Mondal, S. Zou, M. F. Kircher, "DNA-enabled rational design of fluorescence-Raman bimodal nanoprobes for cancer imaging and therapy," *Nat. Commun.* **10**, 1926 (2019).
121. A. Aderem, D. M. Underhill, "Mechanisms of phagocytosis in macrophages," *Annu. Rev. Immunol.* **17**, 593–623 (1999).
122. S. L. Schmid, "Clathrin-coated vesicle formation and protein sorting: An integrated process," *Annu. Rev. Biochem.* **66**, 511–548 (1997).
123. S. D. Conner, S. L. Schmid, "Regulated portals of entry into the cell," *Nature* **422**, 37–44 (2003).
124. J. A. Swanson, C. Watts, "Macropinocytosis," *Trends Cell Biol.* **5**, 424–428 (1995).
125. J. Yao, Y. Fan, Y. Li, L. Huang, "Strategies on the nuclear-targeted delivery of genes," *J. Drug Target.* **21**, 926–939 (2013).
126. A. B. Hill, M. Chen, C.-K. Chen, B. A. Pfeifer, C. H. Jones, "Overcoming gene-delivery hurdles: Physiological considerations for nonviral vectors," *Trends Biotechnol.* **34**, 91–105 (2016).
127. W.-F. Lai, W.-T. Wong, "Design of polymeric gene carriers for effective intracellular delivery," *Trends Biotechnol.* **36**, 713–728 (2018).
128. M. P. Stewart, R. Langer, K. F. Jensen, "Intracellular delivery by membrane disruption: Mechanisms, strategies, and concepts," *Chem. Rev.* **118**(16), 7409–7531 (2018).
129. C. Roma-Rodrigues, L. Rivas-García, P. V. Baptista, A. R. Fernandes, "Gene therapy in cancer treatment: Why go nano?" *Pharmaceutic.* **12**(3), 233 (2020).
130. R. Huschka, A. Barhoumi, Q. Liu, J. A. Roth, L. Ji, N. J. Halas, "Gene silencing by gold nanoshell-mediated delivery and laser-triggered release of antisense oligonucleotide and siRNA," *ACS Nano* **6**, 7681–7691 (2012).
131. L. A. Dykman, N. G. Khlebtsov, "Multifunctional gold-based nanocomposites for theranostics," *Biomaterials* **108**, 13–34 (2016).
132. S. Wang, Y. Chen, S. Wang, P. Li, C. A. Mirkin, O. K. Farha, "DNA-functionalized metal–organic framework nanoparticles for intracellular delivery of proteins," *J. Am. Chem. Soc.* **141**(6), 2215–2219 (2019).
133. I. Lostalé-Seijo, J. Montenegro, "Synthetic materials at the forefront of gene delivery," *Nat. Chem.* **2**, 258–277 (2018).
134. R. Lévy, U. Shaheen, Y. Cesbron, V. Sée, "Gold nanoparticles delivery in mammalian live cells: A critical review," *Nano Rev.* **1**(1), 4889 (2010).
135. S. Aghamiri, A. A. Ghavidel, F. Zandsalimi, S. Masoumi, N. H. Hafshejani, V. Jajarmi, "Nanoparticles-mediated CRISPR/Cas9 delivery: Applications in cancer treatment and detection," *J. Drug. Deliv. Sci. Technol.* **56**, 101533 (2020).
136. C. Richter, J. T. Chang, P. C. Fineran, "Function and regulation of clustered regularly interspaced short palindromic repeats (CRISPR)/CRISPR associated (Cas) systems," *Viruses* **4**(10), 2291–2311 (2012).
137. H. Mollanoori, S. Teimourian, "Therapeutic applications of CRISPR/Cas9 system in gene therapy," *Biotechnol. Lett.* **40**(6), 907–914 (2018).
138. Y. Duan, G. Ma, X. Huang, P. A. D'Amore, F. Zhang, H. Lei, "The CRISPR/CAS9-created *MDM2* T309G enhances vitreousinduced expression of *MDM2* and proliferation and survival of cells," *J. Biol. Chem.* **291**(31), 16339–16347 (2016).
139. S. Chira, D. Gulei, A. Hajitou, A. A. Zimta, P. Cordelier, I. Berindan-Neagoe, "CRISPR/Cas9: transcending the reality of genome editing," *Mol. Ther. Nucl. Acids* **7**, 211–222 (2017).
140. J. Ren, Y. Zhao, "Advancing chimeric antigen receptor T cell therapy with CRISPR/Cas9," *Protein Cell* **8**, 634–643 (2017).
141. S. Lin, B. T. Staahl, R. K. Alla, J. A. Doudna, "Enhanced homology-directed human genome engineering by controlled timing of CRISPR/Cas9 delivery," *Elife* **3**, e04766 (2014).
142. G. J. Gibson, M. Yang, "What rheumatologists need to know about CRISPR/Cas9," *Nat. Rev. Rheumatol.* **13**, 205–216 (2017).
143. P. Wang, L. Zhang, Y. Z. Xie, N. Wang, R. Tang, W. Zheng, X. Jiang, "Genome editing for cancer therapy: Delivery of Cas9 protein/sgRNA plasmid via a gold nanocluster/lipid core–shell nanocarrier," *Adv. Sci.* **4**(11), 1700175 (2017).
144. R. Mout, M. Ray, G. Y. Tonga, Y.-W. Lee, T. Tay, K. Sasaki, V. M. Rotello, "Direct cytosolic delivery of CRISPR/Cas9-ribonucleoprotein for efficient gene editing," *ACS Nano* **11**(3), 2452–2458 (2017).
145. P. Wang, L. Lin, Z. Guo, J. Chen, H. Tian, X. Chen, H. Yang, "Highly fluorescent gene carrier based on Ag–Au alloy nanoclusters," *Macromol. Biosci.* **16**, 160–167 (2016).
146. C. Sardoa, B. Bassib, E. F. Craparoa, C. Scialabbaa, E. Cabrinib, G. Dacarrob, A. D'Agostinob,

A. Tagliettib, G. Giammonaa, P. Pallavicinib, G. Cavallaroa, "Gold nanostar–polymer hybrids for siRNA delivery: Polymer design towards colloidal stability and *in vitro* studies on breast cancer cells," *Int. J. Pharm.* **519**, 113–124 (2017).

147. M. C. Durán, S. Willenbrock, A. Barchanski, J.-M. V. Müller, A. Maiolini, J. T. Soller, S. Barcikowski, I. Nolte, K. Feige, H. M. Escobar, "Comparison of nanoparticle-mediated transfection methods for DNA expression plasmids: Efficiency and cytotoxicity," *J. Nanobiotechnol.* **9**, 47 (2011).
148. B. Du, X. Gu, X. Han, G. Ding, Y. Wang, D. Li, E. Wang, J. Wang, "Lipid-coated gold nanoparticles functionalized by folic acid as gene vectors for targeted gene delivery *in vitro* and *in vivo*," *Chem. Med. Chem.* **12**(21), 1768–1775 (2017).
149. A. Zhang, S. Pan, Y. Zhang, J. Chang, J. Cheng, Z. Huang, T. Li, C. Zhang, J. Martinez de la Fuentea, Q. Zhang, D. Cui, "Carbon-gold hybrid nanoprobes for real-time imaging, photothermal/photodynamic and nanozyme oxidative therapy," *Theranostics* **9**(12), 3443–3458 (2019).
150. K. Lee, M. Conboy, H. M. Park, F. Jiang, H. J. Kim, M. A. Dewitt, V. A. Mackley, K. Chang, A. Rao, C. Skinner, T. Shobha, M. Mehdipour, H. Liu, W.-C. Huang, F. Lan, N. L. Bray, S. Li, J. E. Corn, K. Kataoka, J. A. Doudna, I. Conboy, N. Murthy, "Nanoparticle delivery of Cas9 ribonucleoprotein and donor DNA *in vivo* induces homology-directed DNA repair," *Nat. Biomed. Eng.* **1**, 889–901 (2017).
151. H. Chen, Y. Fan, X. Hao, C. Yang, Y. Peng, R. Guo, X. Shi, X. Cao, "Adoptive cellular immunotherapy of tumors via effective CpG delivery to dendritic cells using dendrimer-entrapped gold nanoparticles as a gene vector," *J. Mater. Chem. B* **8**, 5052–5063 (2020).
152. E. Shaabani, M. Sharifiaghdam, H. De Keersmaecker, R. De Rycke, S. De Smedt, R. Faridi-Majidi, K. Braeckmans, J. C. Fraire, "Layer by layer assembled chitosan-coated gold nanoparticles for enhanced siRNA delivery and silencing," *Int. J. Mol. Sci.* **22**(2), 831 (2021).
153. R. Xiong, S. K. Samal, J. Demeester, A. G. Skirtach, S. C. De Smedt, K. Braeckmans, "Laser-assisted photoporation: Fundamentals, technological advances and applications," *Adv. Phys.: X* **1**, 596–620 (2016).
154. L. Wayteck, R. Xiong, K. Braeckmans, S. C. De Smedt, K. Raemdonck, "Comparing photoporation and nucleofection for delivery of small interfering RNA to cytotoxic T cells," *J. Control. Release.* **267**, 154–162 (2017).
155. S. Courvoisier, N. Saklayen, M. Huber, J. Chen, E. D. Diebold, L. Bonacina, J.-P. Wolf, E. Mazur, "Plasmonic tipless pyramid arrays for cell poration," *Nano Lett.* **2015**(7), 4461–4466 (2015).
156. Z. Lyu, F. Zhou, Q. Liu, H. Xue, Q. Yu, H. Chen, "A universal platform for macromolecular delivery into cells using gold nanoparticle layers via the photoporation effect," *Adv. Funct. Mater.* **26**(32), 5787–5795 (2016).
157. J. Wu, H. Xue, Z. Lyu, Z. Li, Y. Qu, Y. Xu, L. Wang, Q. Yu, H. Chen, "Intracellular delivery platform for "Recalcitrant" cells: When polymeric carrier marries photoporation," *ACS Appl. Mater. Interfaces* **9**(26), 21593–21598 (2017).
158. D. Lapotko, "Plasmonic nanoparticle-generated photothermal bubbles and their biomedical applications," *Nanomedicine* **4**, 813–845 (2009).
159. E. Y. Lukianova-Hleb, A. Belyanin, S. Kashinath, X. Wu, D. O. Lapotko, "Plasmonic nanobubble-enhanced endosomal escape processes for selective and guided intracellular delivery of chemotherapy to drug-resistant cancer cells," *Biomaterials* **33**, 1821–1826 (2012).
160. E. Y. Lukianova-Hleb, M. B. Mutonga, D. O. Lapotko, "Cell-specific multifunctional processing of heterogeneous cell systems in a single laser pulse treatment," *ACS Nano* **6**, 10973–10981 (2012).
161. R. Xiong, F. Joris, S. Liang, R. De Rycke, S. Lippens, J. Demeester, A. Skirtach, K. Raemdonck, U. Himmelreich, S. C. De Smedt, "Cytosolic delivery of nanolabels prevents their asymmetric inheritance and enables extended quantitative *in vivo* cell imaging," *Nano Lett.* **16**, 5975–5986 (2016).
162. R. Xiong, P. Verstraelen, J. Demeester, A. G. Skirtach, J.-P. Timmermans, S. C. De Smedt, W. H. De Vos, K. Braeckmans, "Selective labeling of individual neurons in dense cultured networks with nanoparticle-enhanced photoporation," *Front. Cell Neurosci.* **12**, 80 (2018).
163. P. Chakravarty, C. D. Lane, T. M. Orlando, M. R. Prausnitz, "Parameters affecting intracellular delivery of molecules using laser-activated carbon nanoparticles," *Nanomedicine* **12**(4), 1003–1011 (2016).
164. G. Bisker, D. Yelin, "Noble-metal nanoparticles and short pulses for nanomanipulations: theoretical analysis," *J. Opt. Soc. Am. B* **29**, 1383–1393 (2012).
165. Y. Pan, S. Neuss, A. Leifert, M. Fischler, F. Wen, U. Simon, G. Schmid, W. Brandau, W. Jahnen-Dechent, "Size-dependent cytotoxicity of gold nanoparticles," *Small* **3**, 1941–1949 (2007).
166. N. M. Schaeublin, L. K. Braydich-Stolle, A. M. Schrand, J. M. Miller, J. Hutchison, J. J. Schlager, S. M. Hussain, "Surface charge of gold nanoparticles mediates mechanism of toxicity," *Nanoscale* **3**, 410–420 (2011).

167. R. Lachaine, É. Boulais, M. Meunier, "From thermo- to plasma-mediated ultrafast laser-induced plasmonic nanobubbles," *ACS Photonics* **1** (4), 331–336 (2014).
168. E. Boulais, R. Lachaine, M. Meunier, "Plasma mediated off-resonance plasmonic enhanced ultrafast laser-induced nanocavitation," *Nano Lett.* **12**, 4763–4769 (2012).
169. J. Liu, R. Xiong, T. Brans, S. Lippens, E. Parthoens, F. C. Zanacchi, R. Magrassi, S. K. Singh, S. Kurungot, S. Szunerits, "Repeated photoporation with graphene quantum dots enables homogeneous labeling of live cells with extrinsic markers for fluorescence microscopy," *Light: Sci. Appl.* **7**, 47–57 (2018).
170. T. Pylaev, E. Vanzha, E. Avdeeva, B. Khlebtsov, N. Khlebtsov, "A novel cell transfection platform based on laser optoporation mediated by Au nanostar layers," *J. Biophotonics* **12**(1), e201800166 (2019).
171. M. Gai, M. A. Kurochkin, D. Li, B. N. Khlebtsov, L. Dong, N. Tarakina, R. Poston, D. J. Gould, J. Frueh, G. B. Sukhorukov, "*In-situ* NIR-laser mediated bioactive substance delivery to single cell for EGFP expression based on biocompatible microchamber-arrays," *J. Control. Release* **276**, 84–92 (2018).
172. N. Saklayen, M. Huber, M. Madrid, V. Nuzzo, D. I. Vulis, W. Shen, J. Nelson, A. A. McClelland, A. Heisterkamp, E. Mazur, "Intracellular delivery using nanosecond-laser excitation of large-area plasmonic substrates," *ACS Nano* **11**, 3671–3680 (2017).
173. M. Schomaker, D. Heinemann, S. Kalies, S. Willenbrock, S. Wagner, I. Nolte, T. Ripken, H. M. Escobar, H. Meyer, A. Heisterkamp, "Characterization of nanoparticle mediated laser transfection by femtosecond laser pulses for applications in molecular medicine," *J. Biophotonics* **13**, 10 (2015).
174. A. M. Wilson, J. Mazzaferri, E. Bergeron, S. Patskovsky, P. Marcoux-Valiquette, S. Costantino, P. (Mike) Sapieha, M. Meunier, "*In vivo* laser-mediated retinal ganglion cell optoporation using KV1.1 conjugated gold nanoparticles," *Nano Lett.* **18**(11), 6981–6988 (2018).
175. S. Batabyal, S. Gajjeraman, K. Tchedre, A. Dibas, W. Wright, S. Mohanty, "Near-Infrared Laser-Based Spatially Targeted Nano-enhanced Optical Delivery of Therapeutic Genes to Degenerated Retina," *Mol. Ther.- Methods Clin. Dev.* **17**, 758–770 (2020).
176. E. Lestrell, F. Patolsky, N. H. Voelcker, R. Elnathan, "Engineered nano-bio interfaces for intracellular delivery and sampling: Applications, agency and artefacts," *Mater. Today* **33**, 87–104 (2019).
177. Y.-C. Wu, T.-H. Wu, D. L. Clemens, B.-Y. Lee, X. Wen, M. A. Horwitz, M. A. Teitell, P.-Y. Chiou, "Massively parallel delivery of large cargo into mammalian cells with light pulses," *Nat. Methods* **12**, 439–444 (2015).
178. M. Madrid, N. Saklayen, W. Shen, M. Huber, N. Vogel, E. Mazur, "Laser-activated self-assembled thermoplasmonic nanocavity substrates for intracellular delivery," *ACS Appl. Bio Mater.* **1**(6), 1793–1799 (2018).
179. L. Wang, J. Wu, Y. Hu, C. Hu, Y. Pan, Q. Yu, H. Chen, "Using porous magnetic iron oxide nanomaterials as a facile photoporation nanoplatform for macromolecular delivery," *J. Mater. Chem.* **6**, 4427–4436 (2018).
180. G. C. Messina, M. Dipalo, R. La Rocca, P. Zilio, V. Caprettini, R. P. Zaccaria, A. Toma, F. Tantussi, L. Berdondini, F. De Angelis, "Spatially, temporally, and quantitatively controlled delivery of broad range of molecules into selected cells through plasmonic nanotubes," *Adv. Mater.* **27**(44), 7145–7149 (2015).
181. Kurata, M. Tsukakoshi, T. Kasuya, Y. Ikawa, "The laser method for efficient introduction of foreign DNA into cultured cells," *Exp. Cell Res.* **162**(2), 372–378 (1986).
182. Tirlapur, K. König, "Targeted transfection by femtosecond laser," *Nature* **418**, 290–291 (2002).
183. I. Clark, E. G. Hanania, J. Stevens, M. Gallina, A. Fieck, R. Brandes, B. O. Palsson, M. R. Koller, "Optoinjection for efficient targeted delivery of a broad range of compounds and macromolecules into diverse cell types," *J. Biomed. Opt.* **11**(1), 014034 (2006).
184. M. Leia, H. Xu, H. Yang, B. Yao, "Femtosecond laser-assisted microinjection into living neurons," *J. Neurosci. Methods* **174**(2), 215–218 (2008).
185. H. A. Rendall, R. F. Marchington, B. B. Praveen, G. Bergmann, Y. Arita, A. Heisterkamp, F. J. Gunn-Moore, K. Dholakia, "High-throughput optical injection of mammalian cells using a Bessel light beam," *Lab Chip* **12**, 4816–4820 (2012).
186. J. Liu, R. Xiong, T. Brans, S. Lippens, E. Parthoens, F. C. Zanacchi, R. Magrassi, S. K. Singh, S. Kurungot, S. Szunerits, "Repeated photoporation with graphene quantum dots enables homogeneous labeling of live cells with extrinsic markers for fluorescence microscopy," *Light: Sci. Appl.* **7**, 47–57 (2018).
187. Z. Lyu, F. Zhou, Q. Liu, H. Xue, Q. Yu, H. A. Chen, "Universal platform for macromolecular deliveryinto cells using gold nanoparticle layers via the photoporation effect," *Adv. Funct. Mater.* **26**(32), 5787–5795 (2016).
188. N. Saklayen, M. Huber, M. Madrid, V. Nuzzo, D. I. Vulis, W. Shen, J. Nelson, A. A. McClelland,

A. Heisterkamp, E. Mazur, "Intracellular delivery using nanosecond-laser excitation of large-area plasmonic substrates," *ACS Nano* **11**, 3671–3680 (2017).

189. N. R. Y. Ho, G. S. Lim, N. R. Sundah, D. Lim, T. P. Loh, H. Shao, "Visual and modular detection of pathogen nucleic acids with enzyme-DNA molecular complexes," *Nat. Commun.* **9**, 3238 (2018).
190. H. Y. Lau, J. R. Botella, "Advanced DNA-based point-of-care diagnostic methods for plant diseases detection," *Front. Plant Sci.* **8**, 2016 (2017).
191. M. Y. C. Wu, M. Y. Hsu, S. J. Chen, D. K. Hwang, T. H. Yen, C. M. Cheng, "Point-of-care detection devices for food safety monitoring: Proactive disease prevention," *Trends Biotechnol.* **35**, 288–300 (2017).
192. P. K. Drain, E. P. Hyle, F. Noubary, K. A. Freedberg, D. Wilson, W. R. Bishai, W. Rodriguez, I. V. Bassett, "Diagnostic point-of-care tests in resource-limited settings," *Lancet Infect. Dis.* **14**, 239–249 (2014).
193. H. Xu, M. Gao, X. Tang, W. Zhang, D. Luo, M. Chen, "Micro/nano technology for next-generation diagnostics," *Small Methods* **4**, 4 (2019).
194. M. Z. Yang, Y. Liu, X. Y. Jiang, "Barcoded point-of-care bioassays," *Chem. Soc. Rev.* **48**, 850–884 (2019).
195. J. S. Gootenberg, O. O. Abudayyeh, M. J. Kellner, J. Joung, J. J. Collins, F. Zhang, "Multiplexed and portable nucleic acid detection platform with Cas13, Cas12a, and Csm6," *Science* **360**, 439–444 (2018).
196. C. E. Jin, B. Koo, E. Y. Lee, J. Y. Kim, S. H. Kim, Y. Shin, "Simple and label-free pathogen enrichment via homobifunctional imidoesters using a microfluidic (SLIM) system for ultrasensitive pathogen detection in various clinical specimens," *Biosens. Bioelectron.* **111**, 66–73 (2018).
197. U. Singh, V. Morya, A. Rajwar, A. Richard, C. B. Datta, C. Ghoroi, D. Bhatia, "DNA-functionalized nanoparticles for targeted biosensing and biological applications," *ACS Omega* **5**(48), 30767–30774 (2020).
198. M. Cordeiro, F. F. Carlos, P. Pedrosa, A. Lopez, P. V. Baptista, "Gold nanoparticles for diagnostics: advances towards points of care," *Diagnostics* **6**, 43 (2016).
199. S. Hwu, M. Garzuel, C. Forró, S. J. Ihle, A. M. Reichmuth, F. Kurdzesau, J. Vörös, "An analytical method to control the surface density and stability of DNA-gold nanoparticles for an optimized biosensor," *Colloids Surf. B: Biointerfaces* **187**, 110650 (2020).
200. Z. Yuan, J. Cheng, X. Cheng, Y. He, E. S. Yeung, "Highly sensitive DNA hybridization detection with single nanoparticle flash-lamp darkfield microscopy," *Analyst.* **137**, 2930 (2012).
201. K. Sato, K. Hosokawa, M. Maeda, "Non-cross-linking gold nanoparticle aggregation as a detection method for single-base substitutions," *Nucl. Acids Res.* **33**(1), e4 (2005).
202. H. Li, L. J. Rothberg, "Label-free colorimetric detection of specific sequences in genomic DNA amplified by the polymerase chain reaction," *J. Am. Chem. Soc.* **126**, 10958–10961 (2004).
203. T. E. Pylaev, V. A. Khanadeev, B. N. Khlebtsov, L. A. Dykman, V. A. Bogatyrev, N. G. Khlebtsov, "Colorimetric and dynamic light scattering detection of DNA sequences by using positively charged gold nanospheres: a comparative study with gold nanorods," *Nanotechnology* **22**, 285501 (2011).
204. H. Xu, A. Xia, D. Wang, Y. Zhang, S. Deng, W. Lu, J. Luo, Q. Zhong, F. Zhang, L. Zhou, W. Zhang, Y. Wang, C. Yang, K. Chang, W. Fu, J. Cui, M. Gan, D. Luo, M. Chen, "An ultraportable and versatile point-of-care DNA testing platform," *Sci. Adv.* **6**(17), eaaz7445 (2020).
205. Z. He, H. Yang, "Colourimetric detection of swine-specific DNA for halal authentication using gold nanoparticles," *Food Control.* **88**, 9–14 (2018).
206. H. Kuang, W. Chen, D. Xu, L. Xu, Y. Zhu, L. Liu, H. Chu, C. Peng, C. Xu, S. Zhu, "Fabricated aptamer-based electrochemical "signal-off" sensor of Ochratoxin A," *Biosens. Bioelectron.* **26**, 710–716 (2010).
207. G. Dharanivasan, D. M. I. Jesse, T. Rajamuthuramalingam, G. Rajendran, S. Shanthi, K. Kathiravan, "Scanometric detection of tomato leaf curl New Delhi viral DNA using mono- and bifunctional AuNP-conjugated oligonucleotide probes," *ACS Omega* **4**, 10094–10107 (2019).
208. J. Cheng, L. J. Kricka, *Biochip Technology*, Harwood Academic Publishers, Singapore (2001).
209. P. Keblinski, S. R. Phillpot, S. U. S. Choi, J. A. Eastmen, "Mechanism of heat flow in suspension of nano-sized particles (nanofluids)," *Int. J. Heat Mass Transfer* **45**, 855–863 (2002).
210. M. Hu, G. V. Hartland, "Heat dissipation for Au particles in aqueous solution: relaxation time versus size," *J. Phys. Chem. B* **106**, 7029–7033 (2002).
211. S. Link, C. Burda, Z. L. Wang, M. A. El-Sayed, "Electron dynamics in gold and gold-silver alloy nanoparticles: the influence of a nonequilibrium electron distribution and the size dependence of the electron-phonon relaxation," *J. Chem. Phys.* **111**, 1255–1264 (1999).
212. M. Perner, P. Bost, U. Lemmer, G. von Plessen, J. Feldmann, U. Becker, M. Mennig, M. Schmitt, H. Schmidt, "Optically induced damping of the

surface plasmon resonance in gold colloids," *Phys. Rev. Lett.* **78**, 2192 (1997).
213. J. Z. Zhang, "Ultrafast studies of electron dynamics in semiconductor and metal colloidal nanoparticles: effects of size and surface," *Acc. Chem. Res.* **30**, 423–429 (1997).
214. H. Li, J. Huang, J. Lv, H. An, X. Zhang, Z. Zhang, C. Fan, J. Hu, "Nanoparticle PCR: Nanogold-assisted PCR with enhanced specificity," *Angew. Chem. Int. Ed.* **44**, 5100–5103 (2005).
215. M. Li, Y. C. Lin, C. C. Wu, H. S. Liu, "Enhancing the efficiency of a PCR using gold nanoparticles," *Nucl. Acids Res* **33**, e184 (2005).
216. J. Pan, H. Li, X. Cao, J. Huang, X. Zhang, C. Fan, J. Hu, "Nanogold-assisted multi-round polymerase chain reaction (PCR)," *J. Nanosci. Nanotechnol.* **7**, 4428–4433 (2007).
217. L. J. Mi, H. P. Zhu, X. D. Zhang, J. Hu, C. H. Fan, "Mechanism of the interaction between Au nanoparticles and polymerase in nanoparticle PCR," *Chin. Sci. Bull.* **52**, 2345–2349 (2007).
218. D. X. Cui, F. R. Tian, Y. Kong, I. Titushikin, H. J. Gao, "Effects of single-walled carbon nanotubes on the polymerase chain reaction," *Nanotechnology* **15**, 154–157 (2004).
219. Z. Z. Zhang, M. C. Wang, H. J. An, "An aqueous suspension of carbon nanopowder enhances the efficiency of a polymerase chain reaction," *Nanotechnology* **18**, 355706 (2007).
220. L. Nie, L. Z. Gao, X. Y. Yan, T. H. Wang, "Functionalized tetrapod-like ZnO nanostructures for plasmid DNA purification, polymerase chain reaction and delivery," *Nanotechnology* **18**, 015101 (2007).
221. L. Yuan, Y. He, "Effect of surface charge of PDDA-protected gold nanoparticles on the specificity and efficiency of DNA polymerase chain reaction," *Analyst* **138**, 539–545 (2013).
222. L. Cavigli, B. N. Khlebtsov, S. Centi, N. G. Khlebtsov, R. Pini, F. Ratto, "Photostability of contrast agents for photoacoustics: The case of gold nanorods," *Nanomaterials* **11**, 116 (2021).
223. E. Vanzha, T. Pylaev, V. Khanadeev, S. Konnova, V. Fedorova, N. Khlebtsov, "Gold nanoparticle-assisted polymerase chain reaction: effects of surface ligands, nanoparticle shape and material," *RSC Adv.* **6**, 110146 (2016).
224. R. H. Don, P. T. Cox, B. J. Wainwright, K. Baker, J. S. Mattick, "'Touchdown' PCR to circumvent spurious priming during gene amplification," *Nucl. Acids Res.* **19**, 4008 (1991).
225. Y.-C. Lin, H.-L. Wu, "Nano-PCR: Breaking the bottom limit of the PCR denaturation temperature using nanogold," *TRANSDUCERS and EUROSENSORS '07– Int. Solid-State Sensors, Actuators and Microsystems Conf.*, pp. 391–394, IEEE, Lyon (2007).
226. B. V. Vu, D. Litvinov, R. C. Willson, "Gold nanoparticle effects in polymerase chain reaction: favoring of smaller products by polymerase adsorption," *Anal. Chem.* **80**, 5462–5467 (2008).
227. W. Wan, J. T. W. Yeow, M. I. Van Dyke, "Size-dependent PCR inhibitory effect induced by gold nanoparticles," *Proc. 31st Annual Int. Conf. IEEE Engineering in Medicine and Biology Society: Engineering the Future of Biomedicine*, pp. 2771–2774, IEEE, Minneapolis (2009).
228. A. L. Haber, K. R. Griffiths, Å. K. Jamting, K. R. Emslie, "Addition of gold nanoparticles to real-time PCR: Effect on PCR profile and SYBR Green I fluorescence," *Anal. Bioanal. Chem.* **392**, 887–896 (2008).
229. S.-H. Huang, T.-C. Yang, M.-H. Tsai, I.-S. Tsai, H.-C. Lu, P.-H. Chuang, L. Wan, Y.-J. Lin, C.-H. Lai, C.-W. Lin, "Gold nanoparticle-based RT-PCR and real-time quantitative RT-PCR assays for detection of Japanese encephalitis virus," *Nanotechnology* **19**, 405101 (2008).
230. K. H. Cheong, D. K. Yi, J.-G. Lee, J.-M. Park, M. J. Kim, J. B. Edel, C. Ko, "Gold nanoparticles for one step DNA extraction and real-time PCR of pathogens in a single chamber," *Lab Chip* **8**, 810–813 (2008).